

This thesis is dedicated to my parents who have been so kind and caring to me for the whole of my life. Without their constant motivation and excellent guidance, I could not have imagined reaching this stage. I owe every bit of all my accomplishments to my parents who have always been there to help me with their selfless devotion and love. There is no way to repay all they have done for me over the years. However, this dedication is an expression of my love for them, for they are two of the best souls I have come across in this world.

Abstract

Orthogonal Frequency Division Multiplexing (OFDM) has attracted tremendous attention in the last few years particularly in applications that require high data rates to be supported under fading channels. OFDM has an inherent resistance to multi path components and hence offers critical simplifications in its corresponding single carrier based systems. However, the price of these benefits is paid in the synchronization operations that introduce considerable degradation in performance if not countered appropriately. Timing Synchronization requires the precise location of FFT window to be determined. In addition, the orthogonality of the carriers is frequently disturbed by the fading channel. If this orthogonality is not restored, it introduces Inter Carrier Interference (ICI) and performance is severely compromised.

This work analyses some of the algorithms currently being used to achieve timing and frequency synchronization. These algorithms are extended to high mobility cases where Doppler shift in frequency is another irritant that brings additional fading and degradation. The additional fading produced by the Doppler shift results in a residual error even after a fine frequency estimation scheme. This work proposes a PLL based recovery method which removes this proportional phase shift iteratively for all samples in an OFDM symbol. We determine the imaginary component that remains after a QPSK data point is raised to a power of 4 and this imaginary component is the correction provided to a loop filter that generates the necessary phase correction for the next sample.

We propose a new system level diagram that removes the fine frequency estimation procedure in Minn and Bhargava's estimator and replaces it with our phase recovery scheme. Both systems have been tested under severely degraded channels and our system is found to outperform the one that employs fine frequency estimation. The proposed system, therefore, offers possibilities to support high data rates with a low error probability in a burst mode and at the same time lowers the computational complexity in the overall system.

Acknowledgements

First and foremost, I am really thankful to Allah Almighty, for having given me the courage and adequate physical and mental capacity to produce this thesis. This work could not have reached its present stage without the blessings and boons of Allah. I must thank my advisor, Dr. Shoab Ahmed Khan, for his constant guidance and assistance throughout the duration of this work. I am really grateful for the considerable amount of patience Dr. Shoab has shown in answering my probing queries and doubts. His remarkable motivation and interest during the course of this thesis enabled me to accomplish this task and achieve encouraging results. It was indeed an honor to have fruitful and thought provoking discussions with him and it allowed me to learn a lot about my field of interest.

Some of my friends were also instrumental in helping me produce this work. In particular, I have to mention my friends, Muhammad Azam and Amina Noor, with whom I had many interesting exchanges of thoughts. Their suggestions were quite helpful in stimulating some of my ideas into reality.

I am also indebted to people at Center for Advanced Research in Engineering (CARE) for providing me an excellent work friendly environment. I will remember the exciting days I spent here and the many tasty meals I had at this place.

Table of Contents

CHAPTER 1	1
INTRODUCTION	1
1.1 OUTLINE	3
CHAPTER 2	5
BASIC PRINCIPLES OF OFDM	5
2.1 INTRODUCTION	5
2.2 BASIC SYSTEM MODEL	6
2.3 SPECTRAL EFFICIENCY	9
2.4 SOME DESIGN ELEMENTS	10
2.4.1 <i>Useful Symbol Duration</i>	10
2.4.2 <i>Number of Carriers</i>	10
2.4.3 <i>Modulation Scheme</i>	11
2.4.4 <i>Coded OFDM</i>	11
2.4.5 <i>Length of Guard Interval</i>	11
CHAPTER 3	13
EFFECT OF SYNCHRONIZATION ERRORS	13
3.1 EQUIVALENT SYSTEM MODEL	13
3.2 TIMING AND FREQUENCY SYNCHRONIZATION	14
3.2.1 <i>Effect of a Symbol (or frame) Offset</i>	14
3.2.2 <i>Effect of Carrier Frequency Offset (CFO)</i>	16
CHAPTER 4	19
DATA AIDED SYNCHRONIZATION SCHEMES	19
4.1 SCHMIDL'S TRAINING SYMBOL	20
4.1.1 <i>Designing the Training Symbol</i>	20
4.1.2 <i>Timing Error Estimation</i>	22
4.1.3 <i>Carrier Frequency Offset Estimation</i>	23

4.2	DRAWBACKS OF SCHMIDL'S ALGORITHM	24
4.2.1	<i>Timing Metric Plateau</i>	24
4.2.2	<i>Carrier Frequency Offset Estimation.....</i>	25
4.3	MINN AND BHARGAVA'S IMPROVED ESTIMATOR	26
4.3.1	<i>Training Symbol Formation.....</i>	27
4.3.2	<i>Coarse Timing Estimation</i>	27
4.3.3	<i>Coarse Carrier Frequency Estimation.....</i>	28
4.3.4	<i>Fine Timing Estimation</i>	29
4.3.5	<i>Fine Frequency Estimation.....</i>	29
4.4	DRAWBACKS OF MINN'S IMPROVED ESTIMATOR.....	30
4.4.1	<i>Higher Side lobes</i>	30
4.4.2	<i>Rotation of the Constellation.....</i>	31
CHAPTER 5		34
PHASE RECOVERY MECHANISM.....		34
5.1	THE RESIDUAL ERROR EFFECT	34
5.2	OVERVIEW OF PLL.....	35
5.2.1	<i>Second Order PLL</i>	36
5.3	RECOVERY ALGORITHM.....	37
CHAPTER 6		40
CHANNEL CHARACTERISTICS.....		40
6.1	MOBILE CHANNEL CHARACTERISTICS	40
6.2	FADING DUE TO MULTIPATH EFFECTS	41
6.2.1	<i>Flat Fading</i>	41
6.2.2	<i>Frequency Selective Fading.....</i>	42
6.3	FADING EFFECTS DUE TO DOPPLER SPREAD.....	43
6.3.1	<i>Fast Fading</i>	43
6.3.2	<i>Slow Fading.....</i>	43
6.4	GUIDELINES FOR PRACTICAL SYSTEM IMPLEMENTATION	44
CHAPTER 7		46

PERFORMANCE EVALUATION.....	46
7.1 TRANSMITTER DESIGN	46
7.2 RECEIVER DESIGN	47
7.2.1 <i>Minn and Bhargava:</i>	47
7.2.2 <i>Phase Recovered OFDM</i>	48
7.3 DESIGN PARAMETERS	49
CHAPTER 8.....	56
CONCLUSIONS.....	56
8.1 FURTHER WORK.....	58

List of Figures

FIGURE 2-1 A DISCRETE TIME BASEBAND OFDM SYSTEM	8
FIGURE 2-2 PSD INTO THE CASE OF (A) AN OFDM SIGNAL WITH AN INTERCARRIER.....	9
FIGURE 3-1 SYMBOL TIMING ERRORS	15
FIGURE 3-2 SYMBOL TIMING ERRORS IN A MULTIPATH CHANNEL.....	16
FIGURE 3-3 PSD OF THE OFDM SIGNAL FOR A MULTICARRIER SYSTEM WITH.....	18
FIGURE 4-1 SCHMIDL'S TRAINING SYMBOL	21
FIGURE 4-2 TIMING SYNCHRONIZATION PROCEDURE	23
FIGURE 4-3 PLATEAU INTRODUCED BY SCHMIDL'S TIMING METRIC.....	25
FIGURE 4-4 MINN'S SYNCHRONIZATION SCHEME.....	26
FIGURE 5-1 LINEAR MODEL OF DISCRETE TIME PLL	35
FIGURE 5-2 QPSK CONSTELLATION.....	37
FIGURE 5-3 PHASE RECOVERY MECHANISM	38
FIGURE 7-1 OFDM TRANSMITTER	46
FIGURE 7-2 RECEIVER STRUCTURE FOR MINN'S ALGORITHM.....	47
FIGURE 7-3 RECEIVER WITH PHASE RECOVERY.....	48
FIGURE 7-4 MULTIPATH CHANNEL IMPULSE RESPONSE	50
FIGURE 7-5 WATERFALL.....	50
FIGURE 7-6 TIMING METRIC OBTAINED FOR $L=4$, $L=8$	51
FIGURE 7-7 TIMING OFFSET ESTIMATION	52
FIGURE 7-8 FREQUENCY OFFSET ESTIMATION	53
FIGURE 7-9 PERFORMANCE COMPARISON IN RAYLEIGH FADED CHANNEL. DOPPLER 50 Hz.....	54
FIGURE 7-10 PERFORMANCE COMPARISON IN STATIC RAYLEIGH FADED CHANNEL	55

List of Tables

TABLE 4-1 USE OF PN SEQUENCES FOR SCHMIDL'S TRAINING SYMBOL.....	22
TABLE 4-2 TRAINING SYMBOL SIGN PATTERN	27

Chapter 1

Introduction

Orthogonal Frequency Division Multiplexing (OFDM) has been in place since the early 1960's when a principle for multi channel transmission over a band limited channel was proposed [1]. This proposal was followed by an analysis of the parallel system [2]. The sinusoids required for modulation and demodulation were produced through a DFT implementation in baseband [3]. Further research was carried on this new multi carrier transmission technique and Peled [4] introduced the idea of cyclic redundancy through the use of a cyclic prefix. Although the ground work was laid many years ago, OFDM has emerged as the new modulation technique in the last decade mainly due to advancements made in the DSP implementation of the DFT. OFDM has sparked considerable interest in modern communication systems primarily because of its ability to combat multi path distortions and deliver high data rates at the same time. Dispersive channels pose problems of intersymbol interference (ISI) which degrades the performance of communication systems. OFDM counters this problem through its inherent multi path rejection properties and does so with low computational complexity as compared to its single carrier counterparts. In particular, costly equalizers needed in single carrier systems are dramatically simplified or even obsolete in case differential modulation schemes are used. It is for this reason that OFDM has found use in some of the modern day communication techniques employed round the world. For broadcasting systems, two pertinent examples are Digital Audio Broadcasting (DAB) [17] and Digital Video Broadcasting (DVB) [18]. OFDM is also employed in Wireless Local Area Networks (WLAN) such as IEEE 802.11a and HiperLAN/2. Wireless Metropolitan Area Networks (WMAN) like IEEE 802.16 (WiMax) also uses OFDM as the modulation technique to cater for the degradations caused by the multi path channel dispersions.

While there are a number of advantages that have increased interest in OFDM systems in recent years, there are certain drawbacks that have checked its surge in growth as the technique of

choice. The major drawback is the non ideality between the transmitter and the receiver oscillators. Several studies have been carried out to quantize these synchronization errors that affect the performance of an OFDM transmission system [5], [6]. Speth et.al [7] have reported the factors that can affect the receiver design in an OFDM system. Imperfect channel estimate, symbol or frame offset, carrier and sampling clock frequency offsets and analog components are some of the factors due to which efficiency of OFDM is severely compromised. Specifically, incorrect timing synchronization can cause interference between successive symbols and, if not perfectly compensated before the equalization process, can lead to severe performance degradation. In addition, a carrier-frequency offset (CFO) induces an amplitude reduction of the useful signal and provokes interference between adjacent subcarriers (ICI).

A lot of research has been devoted to the estimation of the design parameters that can help in alleviating the drawbacks associated with OFDM. Blind synchronization algorithms use the statistical properties of the transmitted signal to estimate these parameters of interest. An efficient blind techniques that takes advantage of temporal redundancy induced by the cyclic prefix (CP) has been exploited in [8] to obtain a low complexity estimator. In particular, J.J. van de Beek *et al.* in [8] derive the joint symbol timing and CFO maximum likelihood (ML) estimator under the assumption of a non dispersive channel and by modeling the OFDM signal vector as a circular complex Gaussian random vector (C-CGRV) [9]. The Gaussian assumption is reasonable when the number of subcarriers is sufficiently large. On the other hand, if the length of the cyclic prefix is low, as is the case frequently, this technique does not produce the required results since the cyclic prefix is corrupted by the channel. The correlation based on the cyclic prefix fails to deliver the required information.

Data Aided Estimation techniques have also been used for estimating the synchronization parameters. Different training sequences, whose knowledge is common to both transmitter and receiver, have been employed to synchronize an OFDM systems corrupted by dispersive channels. In particular, in [10] Schmidl and Cox consider a timing and CFO synchronization scheme that exploits the redundancy associated with a training symbol composed by two identical halves. However, the considered timing metric reaches a plateau that produces large variance for the timing estimates. The training symbol proposed in [11], with four identical parts

and a sign inversion, provides a timing metric with steeper roll off. Nevertheless, the sign inversion in the transmitted training symbol introduces, in dispersive channels, some interference in the frequency estimation process causing severe performance degradation. This drawback is investigated by Bhargava et al. in [12] where a more general synchronization algorithm based on a structured training sequence is proposed and, moreover, channel estimation is also incorporated in order to obtain fine timing and CFO estimates. This refinement step reduces the interference introduced in the coarse CFO acquisition process but at the cost of some increase in computational load.

This thesis investigates some of these techniques to estimate the synchronization parameters for an optimum performance. In particular, algorithms [10]-[12] have been simulated for performance comparisons and efficiency over a Rayleigh faded multi path channel that is corrupted by severe delay and Doppler spreads, as is the case with modern day wireless channels. Although the scheme in [12] was found to outperform others, one important drawback is that even a minor frequency offset left uncorrected rotates the received constellation and introduces high BER. Bhargava et al. have introduced a fine frequency step that removes the residual interference but the small error remaining gets accumulated as the duration of an OFDM frame (or symbol) increases. We found that a phase recovery scheme is needed to compensate for the phase introduced by the frequency estimation error. We propose to replace the fine frequency estimation block with this phase recovery mechanism thereby, decreasing computational complexity. The system formed with this phase recovery mechanism outperforms the system developed through estimation algorithms in [12] over a variety of channels considered. We have assumed that timing and frequency offsets are the only impairments and sampling is considered ideal in all cases.

1.1 Outline

The organization of this thesis is as follows.

- **Chapter 2** provides an introduction to OFDM in general. It also analyzes the robustness of the OFDM modulation scheme and some of its advantages over single carrier modulation schemes.

- **Chapter 3** briefly explains the timing and frequency synchronization problems in OFDM systems. Quantization of these two impairments is given [7] to analyze the detrimental effects of faulty estimation of these parameters.
- **Chapter 4** looks at some of the data aided techniques currently used for achieving timing and frequency synchronization in OFDM communication systems. In particular, suggestions in [10]-[12] are investigated.
- **Chapter 5** proposes our phase recovery mechanism to cater for the residual error left uncompensated by the estimation techniques suggested earlier. We also propose a new system level block diagram that replaces the fine frequency estimation step in [12] with our phase recovery technique.
- **Chapter 6** describes the wireless channel considered for analysis. The concepts of fading and coherence time are explained followed by some guidelines for practical system implementation.
- **Chapter 7** tests the above data aided techniques in the dispersive channel described in the previous chapter. A new system with our phase recovery mechanism is also tested in the same conditions. Simulations in MATLAB have been used to carry out the comparison between the various algorithms.
- **Chapter 8** provides some conclusions which summarize the major results had outlines future work in this field

Chapter 2

Basic Principles of OFDM

2.1 Introduction

The last few years have seen remarkable growth in the use of OFDM as the modulation technique in modern communication systems [13]. This interest has sparked mainly due to the promise OFDM has shown in delivering high data rates reliably in a multipath environment with considerable ease in receiver complexity. In order to prevent channel distortions, it is an established fact that the symbol duration has to be kept much greater than the delay spread of the channel. For the communication systems in use these days, the signal bandwidth can be much greater than the coherence bandwidth resulting in distortions in the received signal. In order to minimize these distortions, it becomes necessary to use equalizers whose structure increases in complexity as the ratio between delay spread and symbol period increases. The OFDM modulation scheme offers an alternative solution to deal this problem. This modulation technique is a particular application of more general frequency division multiplexing (FDM) technique (also called multicarrier or multitone modulation). Specifically, in an FDM system a single high-rate bit stream is divided into many lower-rate substreams transmitted over parallel subchannels (or subcarriers). If N is the number of such substreams, the rate on each subchannel decreases as a function of the number of subcarriers. Therefore, for a sufficiently large value of N , each subchannel can present a bandwidth less than the channel coherence bandwidth, and then, it will appear flat fading. This implies that in the receiver a very simple equalization system can be used to compensate, for every subchannel, the attenuation and the phase offset induced by the channel. The multicarrier modulation technique is not new, in fact its origin goes back to the end-1950, when multicarrier modulation has been used in military context to realize high speed communication systems, we cite as examples “Kineplex”, “Adeft” and “Kathryn” systems. Nevertheless, at that time, it didn’t have a particular success because of the high implementation

complexity due to the use of analogical devices. Almost 10 years later, in the 1971, Weinstein and Ebert overcame the problem, publishing their pioneering paper [3] about how to implement a multicarrier system with IDFT/DFT. Subsequently, the principle of the multicarrier modulation became the foundation of most current industry standards and in the coming broadband communication era, especially in wireless communication systems through two principal implementation schemes:

- **DMT (Discrete Multitone)** developed for broadband wired applications has been used as modulation technique for high-bit-rate digital subscriber lines (HDSL) [25], asynchronous digital subscriber lines (ADSL) [26] and the most recent very-high-speed digital subscriber lines (VDSL) [27].
- **OFDM** has been exploited in the European digital audio/video broadcasting (DAB [17], DVB [18]) standards and it has been chosen for wireless local area network (WLAN) applications (such as asynchronous transfer mode (ATM) network and IEEE, ETSI and MMAC WLAN standards). OFDM is under investigation for the fourth generation mobile communication systems and for data transmissions with power lines.

2.2 Basic System Model

A basic system model for a baseband OFDM system that assumes no synchronization errors is presented in figure 2.1 In this discrete time baseband system model, the available bandwidth is divided into N subchannels and X_i represents the data point to be transmitted in the i^{th} subchannel. The time domain sequence transmitted is obtained by invoking an Inverse Discrete Fourier Transform (IDFT) of the complex data sequence. The two sequences are hence related by

$$X_i = \sum_{k=0}^{N-1} x_k e^{\frac{-j2\pi ki}{N}} \quad (2.1)$$

The guard interval introduced to counter the delay spread of the channel consists of G sampling periods. In order to ensure orthogonality of the subcarriers at the receiver, it is a common practice to use a guard interval whose duration is greater than the delay spread of the channel.

This assumption will be used throughout this work so that multipath distortions can be handled. The cyclic prefix is made up of a collection of samples from the end of an OFDM symbol. This cyclic prefix is appended at the start of an OFDM symbol to prevent it from mingling with the subsequent symbols in case of continuous transmission. The new vector formed by the addition of the cyclic prefix is related to the transmitted OFDM symbol as

$$x_{pf}(i) = x_{N-G+i} \quad 0 \leq i \leq G-1 \quad (2.2)$$

The duration of an OFDM symbol is T while T_{CP} is the duration of the cyclic prefix. Hence the overall symbol time can be expressed as $T_{sym} = T + T_{CP}$. Since OFDM divides the wideband channel into a number of narrowband subchannels, let h_k represent the k^{th} channel profile. Here the channel profile is assumed to follow a Rayleigh Faded pattern and the channel is assumed to show sufficient correlation over the duration of atleast one OFDM symbol. It will be shown in Chapter 7 how to measure the duration over which the channel will essentially remain constant. The signal after passing through this Rayleigh Faded channel produces an output given by

$$y_i = \sum_{k=0}^G h_k x_{((i-k))_N} + w_i \quad 0 \leq i \leq N-1 \quad (2.3)$$

where $(())_N$ signifies the cyclic shift. The noise impairment introduced by the channel is denoted by w_i in the form of Additive White Gaussian Noise. At the receiver side, the received sequence is demodulated through the use of a DFT operation.

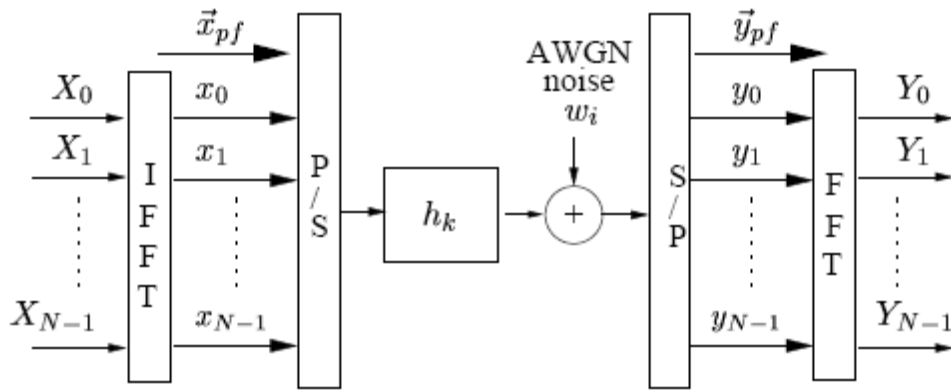


Figure 2-1 A Discrete time baseband OFDM system

The FFT of the received sequence is given by

$$Y_i = H_i X_i + W_i \quad 0 \leq i \leq N - 1 \quad (2.4)$$

As can be seen from the equation, the effect of channel delay spread appears as a multiplication in the frequency domain. It is clear that through the division of a wideband channel into a number of narrowband subchannels, the distortion introduced by the channel is limited to one attenuation and phase change for every subchannel. This is where the advantage of an OFDM system comes in over its single carrier counterpart. As against the complex equalizers used in single carrier transmissions, an OFDM requires a use of single tap equalizers only to retrieve the useful data from the corrupted received sequence. The equalizer in an OFDM system thus takes the form of a multiplier bank only. Differential modulation techniques can be used to render these multiplier banks obsolete as well. However, as the delay spread increases, differential modulation across adjacent sub-bands degrades the performance. We only need to estimate the channel impulse response and use channel inversion to equalize the effect of the dispersive channel.

2.3 Spectral Efficiency

OFDM system offers considerable gain in efficiency when compared with Frequency Division Multiplexing (FDM). The basic system model for OFDM shows that if the carrier in OFDM are spaced by reciprocal of symbol duration T_{sym} , the carrier so formed are orthogonal and do not interfere with each other in ideal conditions. An FDM system on the other hand divides the available bandwidth into a number of frequencies which are not orthogonal and are spaced by some appropriate distance so that they do not overlap. Hence, an OFDM system can pack more carriers in an available bandwidth as compared to an equivalent FDM system.

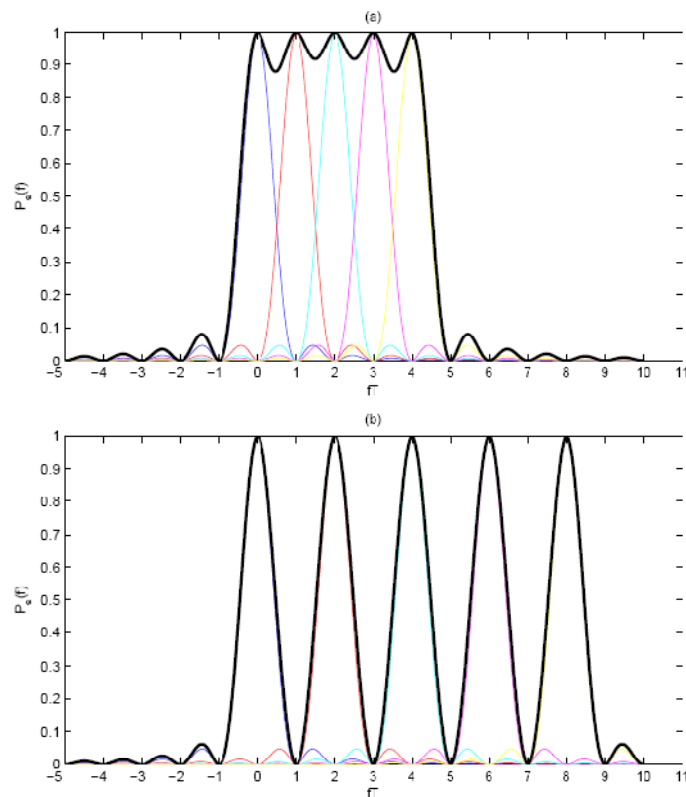


Figure 2-2 PSD into the case of (a) an OFDM signal with an intercarrier spacing $1/T$ and (b) for an FDM signal with an intercarrier spacing $2/T$ [19]

A mathematical analysis of this spectral efficiency has been carried out in [19]. It can be seen from the figure that an OFDM system employs more carriers in any given bandwidth compared to an FDM system and hence can deliver much improved performance.

2.4 Some Design Elements

There are certain elements in OFDM systems that need to be chosen carefully before the actual implementation of the system. An incorrect selection of one of these parameters can lead to a degraded performance of OFDM. Here we look at some of these parameters and see how they are inter-related.

2.4.1 Useful Symbol Duration

The useful symbol duration T_{sym} affects the carrier spacing and coding latency. To maintain the data throughput, a longer useful symbol duration results in an increase in the number of carriers and the size of FFT (assuming that the signal constellation is fixed). In practice, carrier offset and phase stability may affect how close two carriers can be placed. If the application is for the mobile reception, the carrier spacing must be larger enough to make the Doppler shift negligible. Generally the useful symbol duration should be chosen so that the channel remains constant for the duration of at least one symbol.

2.4.2 Number of Carriers

The number of carriers can be determined on the basis of channel bandwidth, data throughput and useful symbol duration. The carriers are spaced by the reciprocal of the useful symbol duration. The number corresponds to the number of complex points being processed in FFT. In HDTV applications, the number of carriers is in several thousands so as to accommodate the data rate and guard interval requirement.

For a given bandwidth, the number of carriers must be chosen so that every subchannel provides only one attenuation and phase change. Thus the wideband channel must be divided into subchannels (which correspond to the number of subcarriers) such that channel is assumed to remain constant in one subchannel. In other words, the bandwidth of each subchannel must be sufficiently smaller than the coherence bandwidth of the channel [20].

$$\frac{BW}{N} \approx CB$$

$$BW = \frac{1}{T_{sym}}$$

$$N \approx \frac{1}{CB * T_{sym}}$$

2.4.3 Modulation Scheme

The modulation scheme used in an OFDM system can be selected based on the requirement of power or spectral efficiency. In general, the selection of modulation scheme applying to each subchannel depends solely on the compromise between the data requirement and transmission robustness. Another advantage of OFDM is that different modulation schemes can be used on different subchannels for layered services.

2.4.4 Coded OFDM

By using time and frequency diversity, OFDM provides a means to transmit data in a frequency selective channel. However, it does not suppress fading itself. Depending on their position in the frequency domain, individual subchannels could be affected by fading. This requires the use of channel coding to further protect the transmitted data. Among those techniques, trellis coded modulation (TCM) combined with frequency and time interleaving is considered the most effective means for a frequency selective fading channel.

2.4.5 Length of Guard Interval

The guard interval appended at the start of an OFDM symbol serves two purposes. It ensures that there is no interference between successive OFDM symbols in a frame i.e. there is no inter-

OFDM-symbol-interference. In addition, if its length is chosen sufficiently longer than the impulse response of the channel, the transient response of the channel dies down within the duration of the guard interval and hence, proceeding symbols in an OFDM frame can be demodulated from the steady state response of the channel. If it is taken as the replica of the data points at the end of an OFDM symbol, it results in the simple multiplication relationship of Eq. 2.4.

The guard interval also decreases the throughput of an OFDM symbol since this information is transmitted as a redundancy associated with the OFDM symbol.

\

Chapter 3

Effect of Synchronization Errors

3.1 Equivalent System Model

A well known problem of OFDM is its high vulnerability to synchronization errors. A lot of research over the years has been devoted to the alleviating the detrimental effect of imperfect synchronization in OFDM communication systems. In a real world system, the following parameters cause disturbances in the receiver [7].

1. The sampling time at the receiver T' can no longer be assumed to be in consonance with the transmitter time T .
2. Carrier frequency offsets result from the same reason while modulating and demodulating the signal. Assuming a small frequency offset relative to the transmission bandwidth, the frequency difference between the transmitter and receiver oscillators can be modeled as a time-variant phase offset at the receiver.
3. The transmitter time scale is unknown to the receiver. Therefore the receiver OFDM window controlling the removal of guard interval will not be identical to an ideal scenario. This timing delay, equivalent to ϵT , can be incorporated in the channel model, resulting in the effective channel $h_{\epsilon,i}$ relevant to the receiver time scale.

All of the effects mentioned are incorporated in an equivalent system model to yield [19]

$$\begin{aligned} r_q(k + \hat{\theta}) &= \sum_{i=-\infty}^{\infty} s(i) e^{j2\pi\Delta f[(k+\hat{\theta})T_c + qT]} \delta[k + qM + \hat{\theta} - \theta - i] \\ &= s_q(k + \Delta\theta) e^{j(\frac{2\pi}{N}\epsilon k + \phi)} \end{aligned} \quad (3.1)$$

3.2 Timing and Frequency Synchronization

This work deals with the timing and carrier frequency synchronization errors only. The sampling offsets are considered negligible and the only channel impairment assumed here is additive noise and time/frequency offsets. The effect of an imperfect estimation of timing and frequency synchronization parameters has been characterized in [19]. Let us first look at the degradation caused by an imperfect estimation of these parameters. The mathematics presented in the following two sections are taken from [19].

3.2.1 Effect of a Symbol (or frame) Offset

In order to see the timing synchronization error degradation, we set $\Delta f = 0$ in Eq. (3.1). The received signal sequence in the presence of noise is

$$r_q(k + \hat{\theta}) = s_q(k + \Delta\theta) + w_q(k + \hat{\theta}) \quad (3.2)$$

After the removal of cyclic prefix and applying the DFT,

$$\tilde{a}_q^l = \sum_{k=0}^{N-1} r_q(k + \hat{\theta}) e^{-j\frac{2\pi}{N}kl} = \sum_{k=0}^{N-1} [s_q(k + \Delta\theta) + w_q(k + \hat{\theta})] e^{-j\frac{2\pi}{N}kl} \quad (3.3)$$

For a timing error that satisfies the condition, $-L_c \leq \Delta\theta \leq 0$, i.e. the timing error stays within the duration of the cyclic prefix, the resulting vector $s_q = [s_q(\Delta\theta), \dots, s_q(N-1+\Delta\theta)]^T$ contains the relevant samples of the q -th OFDM symbol and some algebraic manipulations result in

$$\tilde{a}_q^l = a_q^l e^{j\frac{2\pi}{N}l\Delta\theta} + \eta(l) \quad (3.4)$$

where $\eta(l)$ is the DFT of the noise sequence.

Hence any symbol timing error that is confined to the set $\Delta\theta \in \{-L_c, \dots, 0\}$, the result is only a phase error that can be easily compensated if coherent demodulation is employed at the receiver. A symbol timing error that is not a member of the above defined set, produces interference between consecutive OFDM symbols as the FFT window operation would then be applied on samples taken from two successive OFDM symbols. For a timing error in the interval,

$\Delta\theta \in \{-M, \dots, -L_c\}$, the interference between the successive symbols can be quantized. In this case the (3.3) becomes

$$\begin{aligned} \tilde{a}_q^l &= \frac{M + \Delta\theta}{N} a_q^l e^{j\frac{2\pi}{N}l\Delta\theta} \\ &+ \underbrace{\frac{1}{N} \sum_{k=-\Delta\theta-L_c}^{N-1} e^{-j\frac{2\pi}{N}kl} \sum_{h=0, h \neq l}^{N-1} a_q^h e^{j\frac{2\pi}{N}h(k+\Delta\theta)}}_{ICI} \\ &+ \underbrace{\frac{1}{N} \sum_{k=0}^{-\Delta\theta-L_c} e^{-j\frac{2\pi}{N}kl} \sum_{h=0}^{N-1} a_{q-1}^h e^{j\frac{2\pi}{N}h(k+\Delta\theta)}}_{ISI} + \eta(l) \end{aligned} \quad (3.5)$$

In this case the demodulated signal at the receiver will be corrupted by the ICI and ISI affected samples. The useful portion is still only affected by a phase rotation and can be easily regenerated at the receiver. The interference from the adjacent carriers and from the previous OFDM symbol are the causes of major degradations in a demodulated OFDM symbol.

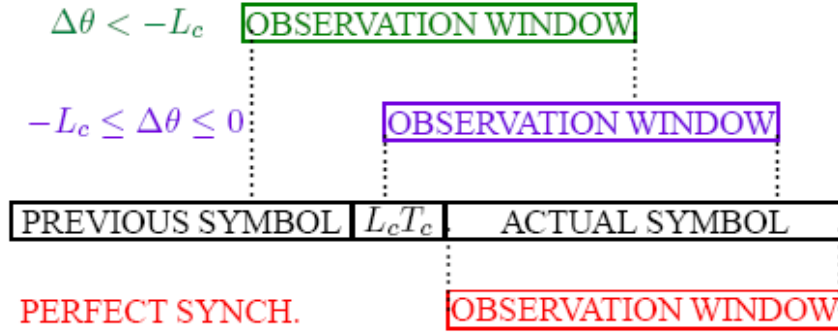


Figure 3-1 Symbol Timing Errors

The same performance degradation can also be carried out for a multipath channel. To this effect, the received signal can be represented by

$$r_q(n) = \sum_{l=0}^{N_m} h(l) s_q(k-l-\theta) + w_q(n) \quad (3.6)$$

where h_l is the multipath channel with a maximum delay spread N_m . The DFT operation is then invoked and the resulting signal can be expressed as

$$\tilde{a}_q^l = \alpha(\theta) a_q^l H(l) e^{-j\frac{2\pi}{N}l\theta} + \xi(l) + \eta(l) \quad (3.7)$$

where $\xi(l)$ models the interference caused by the ISI and ICI degradations. It becomes imperative in this case to synchronize the receiver to the first arriving multipath component. Hence the range for allowable symbol timing offset errors can be expressed by

$$-L_c + N_m \leq \Delta\theta \leq 0$$

i.e. the allowable range for timing errors is limited to that part of the cyclic prefix that has not been corrupted by the channel delay spread. If the timing is locked within this region, the orthogonality between the subcarriers is not disturbed and we only have a phase rotation and attenuation at the DFT output. This can be corrected by the use of a simple equalizer.

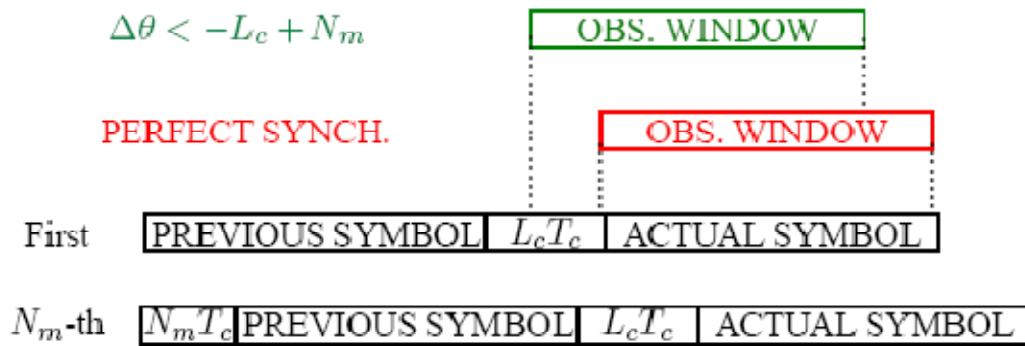


Figure 3-2 Symbol timing errors in a multipath channel

3.2.2 Effect of Carrier Frequency Offset (CFO)

To see the performance loss caused by the CFO, we put $\Delta\theta = 0$ in (3.1). The received signal can then be represented by

$$r_q(n) = s_q(n) e^{j(\frac{2\pi}{N}\epsilon k + \phi)} + w_q(n) \quad (3.8)$$

For a carrier frequency offset that is an integer multiple, the rotation occurs in all the subcarriers and although displaced, they will still remain mutually orthogonal. For a CFO, that is a fraction of the carrier spacing, the demodulated OFDM signal is given by

$$\tilde{a}_q^l = \sum_{k=0}^{N-1} \left[s_q(k) e^{j \left[\frac{2\pi}{N} \epsilon k + \phi \right]} + w_q(k) \right] e^{-j \frac{2\pi}{N} kl} \quad (3.9)$$

Then accounting for the expression of the transmitted signal we have

$$\begin{aligned} \tilde{a}_q^l &= \sum_{k=0}^{N-1} \left[\frac{e^{j \left(\frac{2\pi}{N} \epsilon k + \phi \right)}}{N} \sum_{h=0}^{N-1} a_q^h e^{j \frac{2\pi}{N} hk} + w_q(k) \right] e^{-j \frac{2\pi}{N} kl} \\ &= e^{j \left[\pi \epsilon \left(\frac{N-1}{N} \right) + \phi \right]} \frac{\sin(\pi \epsilon)}{N \sin \left(\frac{\pi \epsilon}{N} \right)} \tilde{a}_q^l \\ &\quad + \underbrace{\frac{e^{j\phi}}{N} \sum_{h=0, h \neq l}^{N-1} a_q^h \sum_{k=0}^{N-1} e^{j \frac{2\pi}{N} k(h-l+\epsilon)}}_{ICI} + \eta(l) \\ &= \frac{e^{j\phi}}{N} a_q^l I_o(\epsilon) + \underbrace{\frac{e^{j\phi}}{N} \sum_{h=0, h \neq l}^{N-1} a_q^h I_{h-l}(\epsilon)}_{ICI} + \eta(l) \end{aligned} \quad (3.10)$$

Where

$$I_p(\epsilon) \square \sum_{k=0}^{N-1} e^{j \frac{2\pi}{N} k(\epsilon+p)} = \frac{\sin \left[\pi (\epsilon+p) \right]}{\sin \left[\frac{\pi}{N} (\epsilon+p) \right]} e^{j \left[\pi \left(\frac{N-1}{N} \right) (\epsilon+p) \right]}$$

The received signal is composed of the attenuated term, the term affected by ICI and the noise disturbance. Figure 3.3 will show the effect of CFO on the originally orthogonal carriers. The PSD of the OFDM signal in the absence of synchronization errors are depicted by solid lines and the dashed lines show the effect of CFO for $\epsilon = 0.2$. It is clear that the presence of CFO produces a reduction in signal amplitude and ICI. The degradation due to CFO in a multicarrier system has been determined analytically in [21]. This performance loss can be approximated in dB as

$$D(\text{dB}) \square \frac{SNR}{SNR_\epsilon(\epsilon)} \square \frac{10(\pi \epsilon)^2 SNR}{3 \ln 10} = \frac{10(\pi \Delta f T_c N)^2}{3 \ln 10}$$

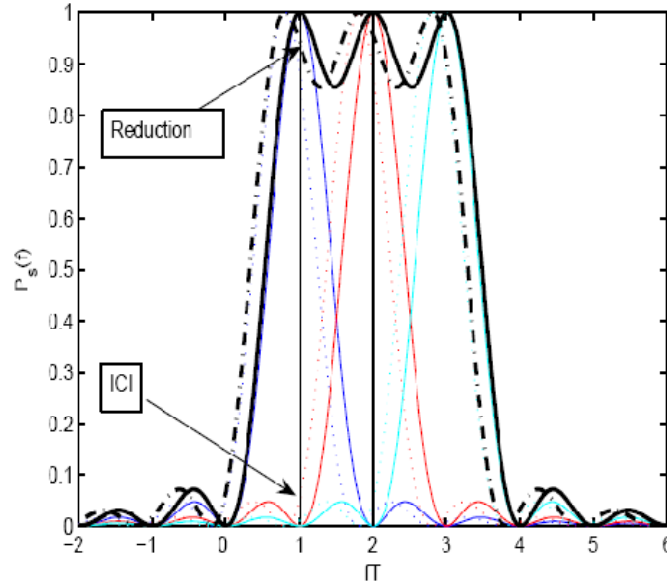


Figure 3-3 PSD of the OFDM signal for a multicarrier system with $N = 3$ subcarriers in presence (dashed lines) and in absence (solid lines) of CFO

It is clear that performance degrades with square of the number of carriers. The same results can be extended to a dispersive channel resulting in the demodulated data given by

$$\tilde{a}_q^l = \frac{e^{j\phi}}{N} a_q^l H(l) I_o(\epsilon) + \underbrace{\frac{e^{j\phi}}{N} \sum_{h=0, h \neq l}^{N-1} a_q^h H(h) I_{h-l}(\epsilon)}_{ICI} + \eta(l) \quad (3.11)$$

The equation indicates that a multipath channel will add attenuation and a carrier phase offset in addition to those introduced by the ICI. Moose has analytically determined the lower bound on the SNR obtained at the output of the DFT as a result of CFO errors [22]

$$SNR_{\epsilon}(\epsilon) \geq \frac{SNR}{1 + 0.5947 SNR \sin^2(\pi \epsilon)} \left(\frac{\sin(\pi \epsilon)}{\pi \epsilon} \right)^2$$

Chapter 4

Data Aided Synchronization Schemes

A number of synchronization schemes have been proposed in the literature to investigate and alleviate the performance loss encountered in an OFDM communication system due to timing and frequency offsets [5]-[12]. These algorithms for synchronization can be divided into two categories

1. Blind Synchronization Techniques

These techniques propose to achieve synchronization without any advance knowledge of the system. They try to estimate the parameters needed for synchronization through the statistical properties of the received signal only. In particular, Van de Beek in [8] has suggested achieving synchronization through the use of cyclic prefix only. However, this algorithm is limited by its high dependence on SNR values the length of cyclic prefix. For a system where the cyclic prefix is not much in duration and is corrupted by the dispersive channel, this technique exhibits an error floor. Some methods have been suggested to determine synchronization through the ISI free part of the cyclic prefix only. But these schemes do not perform well in multipath affected environments.

2. Data Aided Synchronization Techniques

The data aided techniques frequently use a specially designed training symbol whose knowledge is common to both transmitter and receiver. This training symbol is used at the receiver to calculate the variables of interest. Schmidl in [10], Minn and Bhargava in [11],[12] have proposed training symbol structures that aid the synchronization process. These techniques, although quite robust in their performance, result in an increase in computational complexity and throughput is compromised as well.

In this chapter, we evaluate the performance of some data aided techniques proposed in [10]-[12]. A brief look at their algorithm is followed by an analysis of the performance curves. Some of the drawbacks of these techniques are also investigated. This lays down the ground work for our proposal of phase recovery to be discussed in the next chapter.

4.1 Schmidl's Training Symbol

Schmidl et al. proposes a synchronization scheme for both a continuous and burst mode application in OFDM transmission systems. The algorithm proposes modifications of Classen's method which both greatly simplify the computations necessary for synchronization and extend the range for acquisition of carrier frequency offset. By using one unique training symbol, this method can be used for bursts of data to find whether a burst is present and to find the start of the burst. Acquisition is achieved in two simple steps, through the use of a two-symbol training sequence, which is usually appended at the start of an OFDM frame. First the symbol/frame synchronization is determined by searching for this specially designed training symbol. The carrier frequency offset is then partially corrected and a correlation with the second symbol is performed to find the carrier frequency offset.

4.1.1 Designing the Training Symbol

The symbol timing recovery relies on the search of a training symbol which has identical halves in time domain. The two halves of the training symbol essentially remain the same after passing through the channel except for the fact that there will be a phase difference between them. This phase difference is caused by the carrier frequency offset. These two halves of the first training symbol are made identical in the time domain by transmitting PN sequences on the even frequencies. We send zeros on the odd frequencies. The IFFT of such a sequence would result in a time domain signal with two identical halves in the time domain.

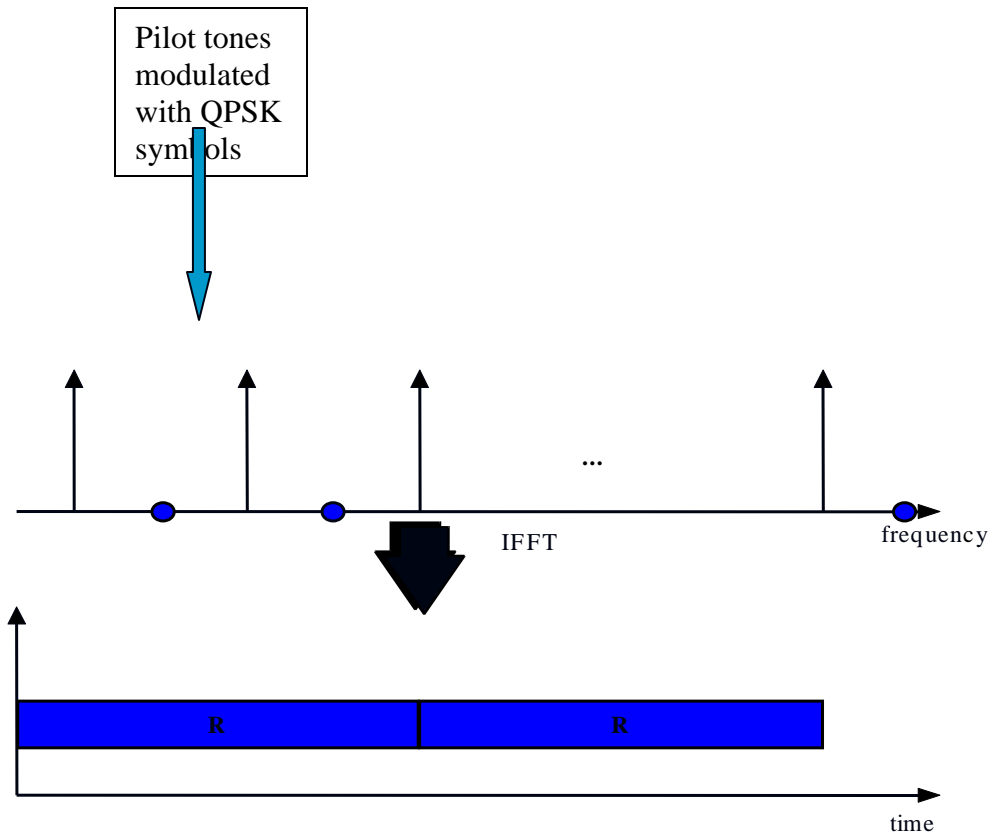


Figure 4-1 Schmid's training symbol

The second training symbol is used for the purpose of calculating integer offsets and is produced by the transmission of PN sequence on the odd frequencies to measure these subchannel and another PN sequence of the even frequencies to help determine the frequency offset. The PN sequence can be selected so as to improve performance and on the basis of producing low Peak to Average Power Ratio (PAPR) values.

Freq. num. k	$c_{1,k}$	$c_{2,k}$	$v_k = \sqrt{2} \frac{c_{2,k}}{c_{1,k}}$
-4	$7+7j$	$5-5j$	$-j$
-3	0	$-5-5j$	
-2	$-7+7j$	$-5-5j$	j
-1	0	$-5+5j$	
0	$7+7j$	$-5-5j$	-1
1	0	$5+5j$	
2	$7-7j$	$-5+5j$	-1
3	0	$5-5j$	
4	$7+7j$	$5+5j$	1

Table 4-1 Use of PN sequences for Schmidl's training symbol

4.1.2 Timing Error Estimation

The first training symbol in which the two halves are identical, except for a phase difference caused by the carrier frequency offset, is used to find the start of the burst. If there are L complex samples in each half, the correlation matrix can be written as

$$P(d) = \sum_{m=0}^{L-1} (r_{d+m}^* r_{d+m+L}) \quad (4.1)$$

where $r(n)$ is the received OFDM signal. Here d is the time index corresponding to the first sample in the received window of $2L$ samples. This window slides along in time as the receiver searches for the first training symbol. The received energy for the second half symbol is defined by

$$R(d) = \sum_{m=0}^{L-1} |r_{d+m+L}|^2 \quad (4.2)$$

A timing metric is then defined based on the correlation matrix calculated previously. This timing metric will be denoted by M_{Sch} to represent Schmidl's timing metric.

It is given by

$$M_{Sch} = \frac{|P(d)|^2}{(R(d))^2} \quad (4.3)$$

The peak of this timing metric signifies the start of the useful part of the training symbol (excluding the cyclic prefix). The precise location of the start of the OFDM frame can then be determined.

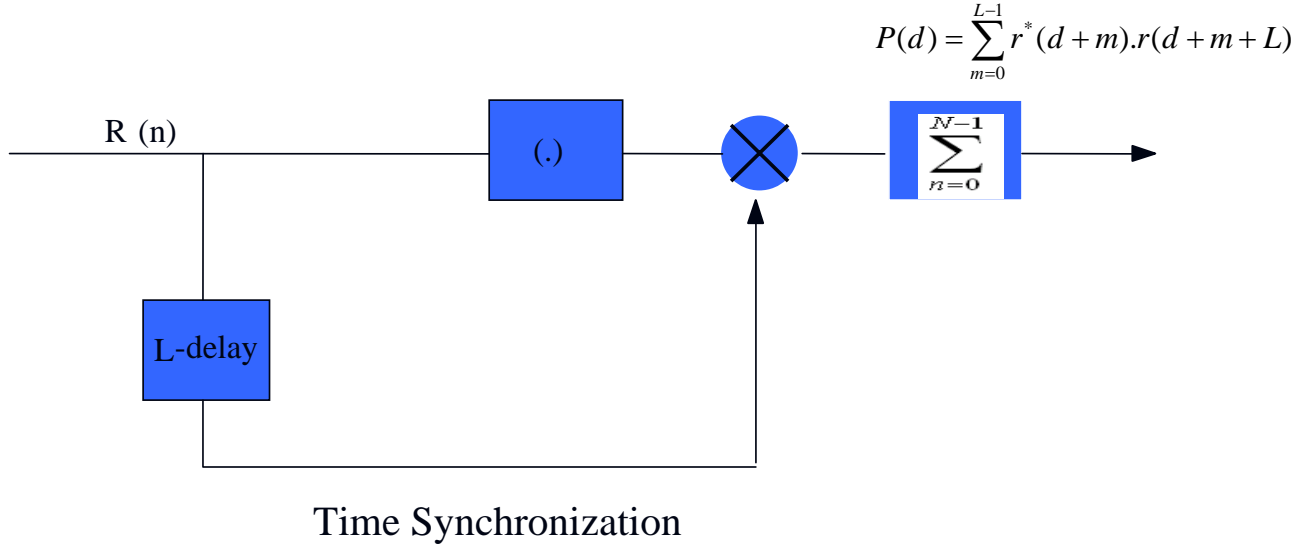


Figure 4-2 Timing synchronization procedure

4.1.3 Carrier Frequency Offset Estimation

The main difference between the two halves of the first training symbol will be a phase difference of

$$\phi = \pi T \Delta f \quad (4.4)$$

This difference in phase can be approximated by

$$\hat{\phi} = \text{angle}(P(d)) \quad (4.5)$$

near the optimum timing point. If $|\hat{\phi}|$ can be guaranteed to be less than π , then the frequency offset estimate is

$$\Delta \hat{f} = \frac{\hat{\phi}}{\pi T}$$

In case there is an integer offset, we will have to use the second training symbol and the method is described in [10].

4.2 Drawbacks of Schmidl's Algorithm

Although Schmidl's technique was one of the first and very useful data aided synchronization methods, it suffers from some performance degradations.

4.2.1 Timing Metric Plateau

A well known problem associated with Schmidl's timing metric is the plateau produced which has a length equal to the length of guard interval minus the length of channel impulse response since there is no ISI within this interval to distort the signal. For frequency selective channels, the length of the impulse response of the channel is shorter than the guard interval by design choice of the guard interval, so the plateau here is shorter as compared to the one for AWGN channels. This plateau introduces uncertainty in the timing metric as the precise peak of the timing metric could be anywhere within this plateau. This uncertainty in turn leads to large timing offset estimate variance.

The figure below shows this plateau for a Rayleigh faded multipath channel with a delay spread of 15 μ s. The exact timing point was located at the 19th sample shown on x-axis. We can see here that there is uncertainty due to the inherent plateau introduced by Schmidl's training symbol.

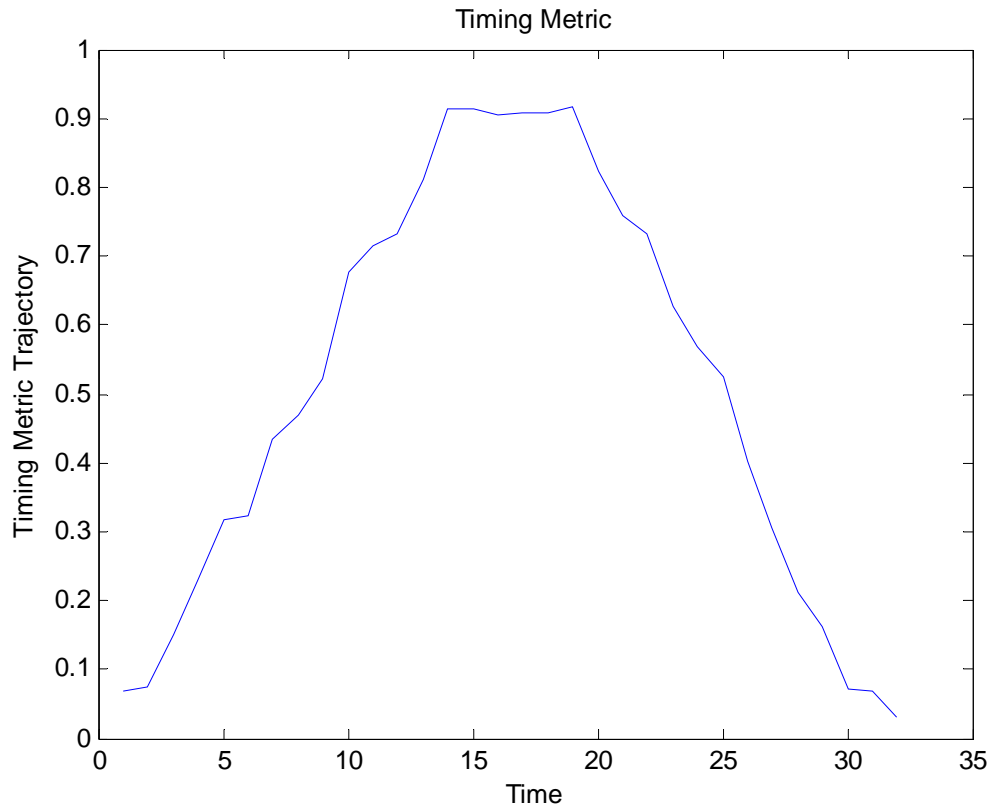


Figure 4-3 Plateau introduced by Schmid's Timing Metric

4.2.2 Carrier Frequency Offset Estimation

Carrier frequency offset estimation too, suffers from large performance variations due to uncertainty associated with the timing metric. If the timing point determined is not accurate, the estimation procedure for carrier frequency suffers adversely. Moreover, if the offset exceeds one carrier spacing, we need another training symbol for its estimation. This decreases the overall throughput of the system. Also there seems to be no mechanism to fine tuning the frequency estimate once it has been found and the resulting error may cause SNR degradation and rotation of the constellation at the receiver.

4.3 Minn and Bhargava's Improved Estimator

Minn and Bhargava proposed an improved and more general synchronizer through the aid of a specially designed training symbol. This method is specifically designed to have a steep roll off timing metric, thus alleviating the main drawback of Schmidl's algorithm. The structure of this estimator is represented by the following figure.

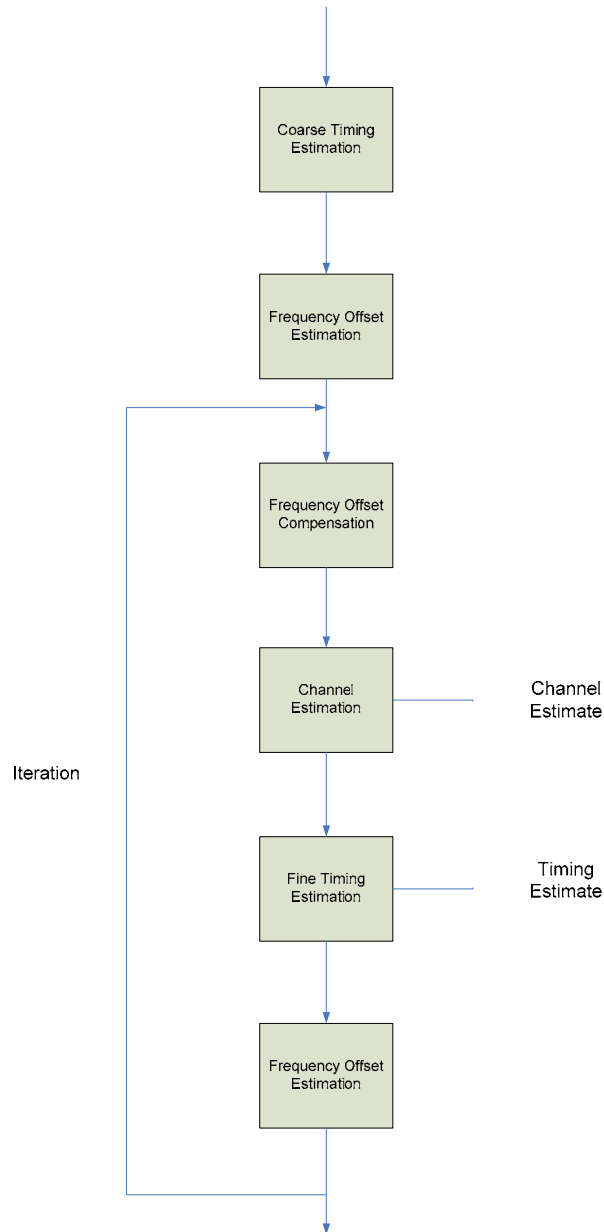


Figure 4-4 Minn's Synchronization Scheme

4.3.1 Training Symbol Formation

The training symbol has been designed both for an OFDM-type Frequency Domain training or single carrier-type Time Domain training. This training symbol is composed of L identical parts to handle the frequency offsets up to $\pm L/2$ carrier spacing. The L identical parts are supplied with specific sign patterns to give a steep roll off timing metric trajectory. The training symbol can be designed with the help of Golay complementary sequences which are known to result in low PAPR values. The basic structure of the training symbol is

$$s = [\pm A, \pm A, \pm A, \dots, \pm A] \quad (4.6)$$

where A is the repeated part which is given a predetermined sign pattern whose knowledge is common to both transmitter and receiver. The sign patterns for different values of L were determined by a computer search and are given in the following table.

L	Sign Pattern
4	(-+—)
	(+++-)
8	(++---+---)
	(-++----+)
16	(+---++++---+---+---)
	(---+++++-----+---)

Table 4-2 Training Symbol Sign Pattern

4.3.2 Coarse Timing Estimation

The coarse timing estimation proceeds in the same way as the one in case of Schmidl and Cox and requires finding the peak of the timing metric defined by the following equations

$$\begin{aligned}
v_{\epsilon}(d) &= \left(\frac{L}{L-1} \frac{|P(d)|}{E(d)} \right)^2 \\
P(d) &= \sum_{k=0}^{L-2} b(k) \sum_{m=0}^{M-1} r^*(d+kM+m).r(d+(k+1)M+m) \\
E(d) &= \sum_{i=0}^{M-1} \sum_{k=0}^{L-1} |r(d+i+kM)|^2
\end{aligned} \tag{4.7}$$

The identical parts would ensure that there is no uncertainty in the timing metric and a sharp peak is obtained. For $L = 2$ this method reduces to the one proposed by Schmidl. We already know that in order to maintain orthogonality, the timing estimate should be in the ISI free part of the cyclic prefix. In multipath channels, the peak of the timing metric is shifted by the mean channel dispersion. Hence the coarse timing estimate should be pre-advanced by some samples λ_c as

$$\hat{\epsilon}_c = d_{\max} - \lambda_c$$

4.3.3 Coarse Carrier Frequency Estimation

The coarse estimation proceeds by using the Morelli and Mengali algorithm with appropriate modifications. The training symbol structure is modified so that all the identical parts have the same sign. This modified training symbol is represented by $\{y(k) : k = 0, 1, \dots, N-1\}$. The coarse estimate is given by

$$\begin{aligned}
R_y(m) &= \frac{1}{N-mM} \sum_{k=mM}^{N-1} y^*(k-mM)y(k), 0 \leq m \leq H \\
\varphi(m) &= \left[\arg\{R_y(m)\} - \arg\{R_y(m-1)\} \right]_{2\pi}, 1 \leq m \leq H \\
w(m) &= 3 \frac{(L-m)(L-m+1) - H(L-H)}{H(4H^2 - 6LH + 3L^2 - 1)} \\
\hat{\nu} &= \frac{L}{2\pi} \sum_{m=1}^H w(m)\varphi(m)
\end{aligned}$$

For multipath dispersive channels, the repeated parts of the training symbol will not be equal due to sign conversion in the transmitted training symbol. The frequency is estimated by restoring equal signs for all the repeated parts but this sign flipping does not improve the impairments

introduced by the frequency selective channel. This explains the need for fine estimation explained later.

4.3.4 Fine Timing Estimation

Coarse timing estimate is before the actual timing point usually due to pre-advancement. We require determining the channel delay to remove the effect of time varying nature of the channel. Hence the coarse estimate can be fine tuned by adding the delay of the first actual channel tap from the channel estimate. The strategy is to determine the strongest tap gain estimate $\hat{h}_{\max} = \max\{\hat{h}_i : i = 0, 1, \dots, K' - 1\}$. The first channel tap delay is given by

$$\begin{aligned} \hat{\tau}_o &= \arg \max_l \{E_h(l) : l = 0, 1, \dots, K^* - K'\} \\ E_h(l) &= \begin{cases} \sum_{k=0}^{K'-1} |\hat{h}_{l+k}|^2, & \text{if } |\hat{h}_l| > \eta |\hat{h}_{\max}| \\ 0 & \end{cases} \end{aligned} \quad (4.8)$$

The fine timing estimate is then determined by

$$\hat{\epsilon} = \hat{\epsilon}_c + \hat{\tau}_o - \lambda_f$$

Where λ_f is the designed pre-advancement to reduce the possible ISI. Without the advancement, the fine timing estimate would be precise most of the time. However, if the ratio of first tap to strongest tap is smaller than η , the most likely chosen channel tap as the first tap would be the second channel tap. Hence λ_f should be a least the delay difference between the first and second taps.

4.3.5 Fine Frequency Estimation

The training symbol pattern introduces some interference in frequency estimation. If this interference is not taken into account in the fine stage, fine frequency estimation will inherit the resulting performance degradation. Minn and Bharagava use an ML estimation scheme to determine this fine frequency offset. This ML estimation is given as

$$\Omega(\hat{\epsilon}_v; \tilde{v}) = r^H(\hat{\epsilon}_v)W(\tilde{v})BW^H(\tilde{v})r(\hat{\epsilon}_v) \quad (4.9)$$

Where $B = S(S^H S)^{-1} S^H$ and S is the matrix obtained in channel estimation. More details of this ML estimation can be found in [12, pg 830].

4.4 Drawbacks of Minn's Improved Estimator

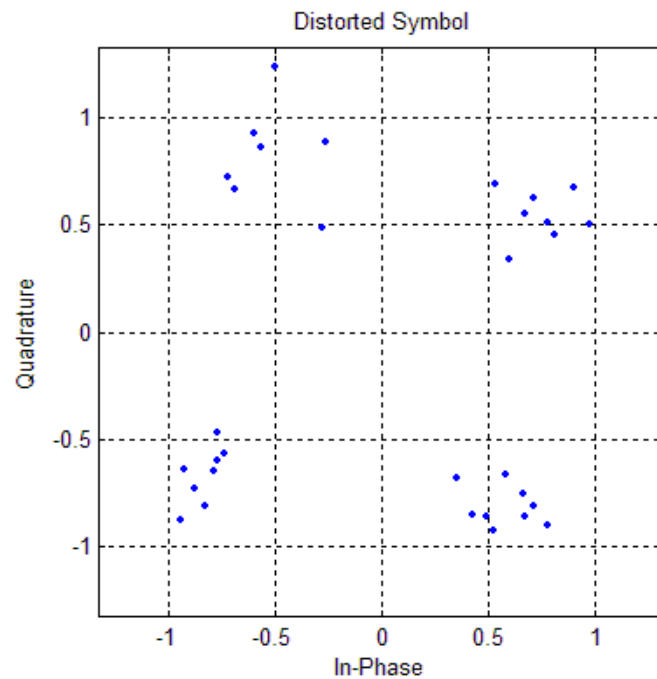
The timing estimator proposed by Minn removes the discrepancies in Schmidl's synchronization strategy. It produces a much sharper timing metric and has a larger estimation range for the carrier frequency offset depending upon the number of repeated parts of the training symbol. It also improves the throughput of the system considerably in comparison to [10] since only one training symbol is used to estimate the correct timing, frequency and channel estimate. In spite of all these advantages, it introduces degradations of its own in an OFDM communication system. We look at two important discrepancies that need to be corrected.

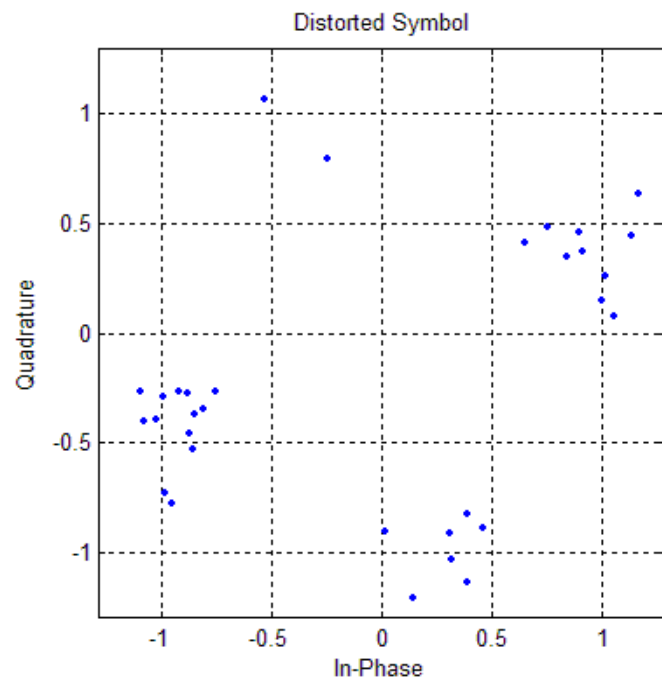
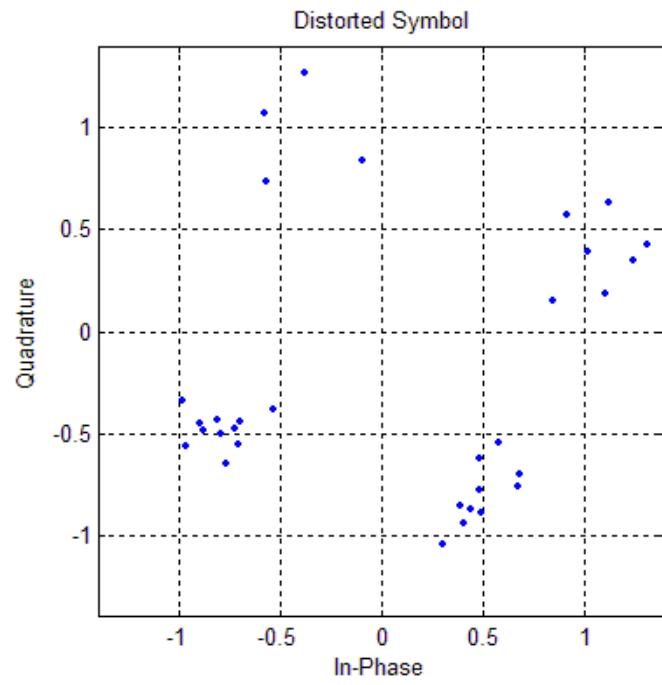
4.4.1 Higher Side lobes

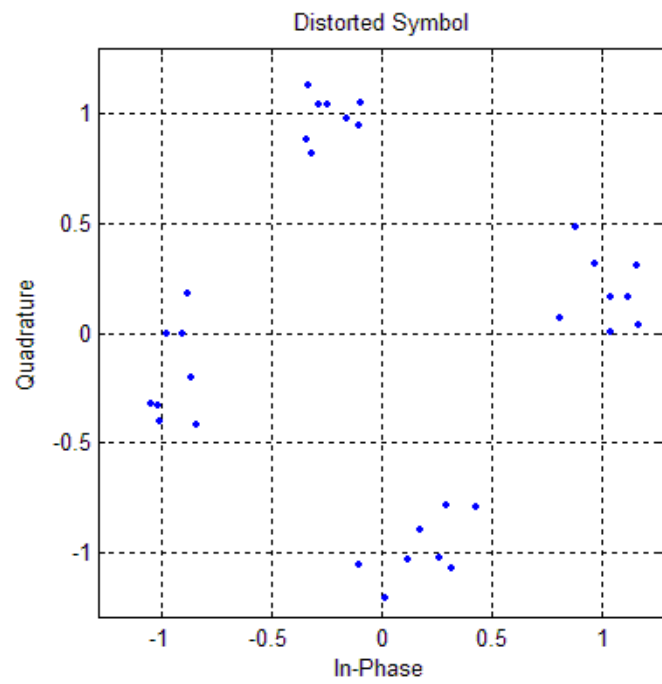
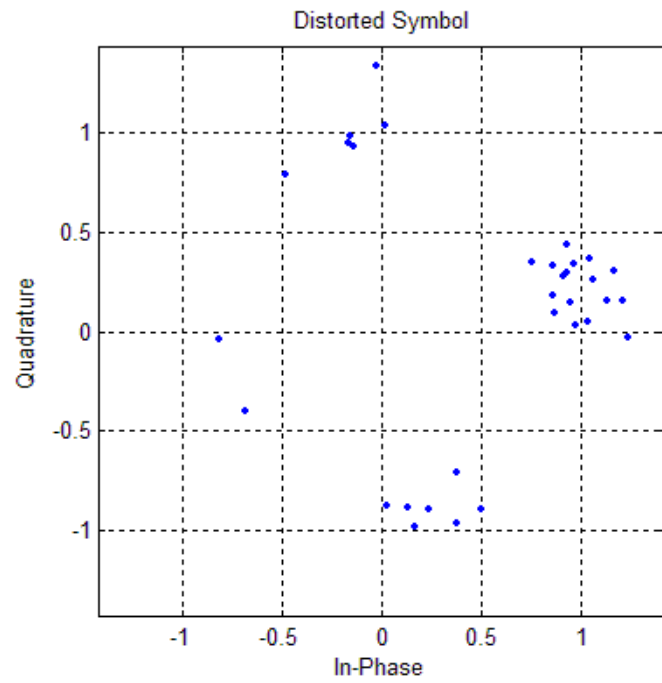
The timing metric produced in this technique is quite robust and performs well in low SNR as well. However for $L=4$, the difference between the peak of the timing metric and the side lobe is small and can easily cause confusion if they are slightly disturbed from their positions. A threshold applied can take the side lobe for the peak of the timing metric if its height is raised a little. The algorithm proposes to use a greater number of identical parts to alleviate this problem. This process does suppress the side lobes but Minn has himself indicated, the greater the number of identical parts, greater will be the resulting interference introduced due to sign conversions. This additional frequency error due to the sign conversions in the design of the training symbol can cause large losses in performance.

4.4.2 Rotation of the Constellation

The algorithm has an impressive range of frequency error correction and employs both coarse and fine stages to determine the frequency offset introduced by the dispersive channel. Since we know that ICI is the cause of large degradations in an OFDM system, the uncorrected frequency error rotates the constellation at the receiver. This error increases with time for subsequent OFDM symbols in a frame and there comes a time when the received constellation crosses its specific quadrants and hence it cannot be decoded by the decision device. A pictorial representation of this effect is shown below.







Chapter 5

Phase Recovery Mechanism

The residual error that remains in the frequency estimation procedure provides a shift to the demodulated OFDM symbol that increases as the samples evolve in time. This error, if left uncompensated, introduces a phase shift in the demodulated data and there may be a chance of the received constellation crossing the respective quadrants. It will not be possible to use hard decoding for a reliable reception. This chapter investigates this residual error and proposes a PLL based recovery scheme that can be used to lock the phase of received OFDM symbols.

5.1 The Residual Error Effect

To analyze the rotating effect due to the residual error on the demodulated data, let us consider a continuous time OFDM signal $x(t)$ that is produced by taking the IFFT of the complex data symbols to be transmitted. The signal received at the receiver can be expressed as

$$y(t) = x(t)e^{j2\pi\theta t} \quad (5.1)$$

where θ is the normalized frequency offset introduced in the transmitted signal. For the moment we consider that timing synchronization has been established and coarse and fine frequency blocks in [12] have been invoked. Let $\hat{\theta}$ be the fine estimate obtained after using the method described in the previous chapter. After compensation the received signal can now be given as

$$y(t) = x(t)e^{j2\pi\theta t} e^{-j2\pi\hat{\theta}t}$$

$$y(t) = x(t)e^{j2\pi(\theta-\hat{\theta})t}$$

$$y(t) = x(t)e^{j2\pi\psi t}$$

where $\psi = \theta - \hat{\theta}$ is the normalized residual error that remained even after the fine frequency estimation stage.

Although the fine estimation procedure works well compared to other contemporary algorithms, it still produces a residual error that must be compensated. Moreover, this error is of the order of carrier spacing and if the carrier spacing is high, this error would be a high figure as well. In many systems, even such a small error can cause large degradations (as would be shown for the case of a practical OFDM system). We explore a second order PLL based recovery scheme for the case of QPSK modulation scheme only.

5.2 Overview of PLL

Let us consider a linear model of the PLL for analysis and subsequent use. The linear model for a discrete time PLL is represented by the following figure.

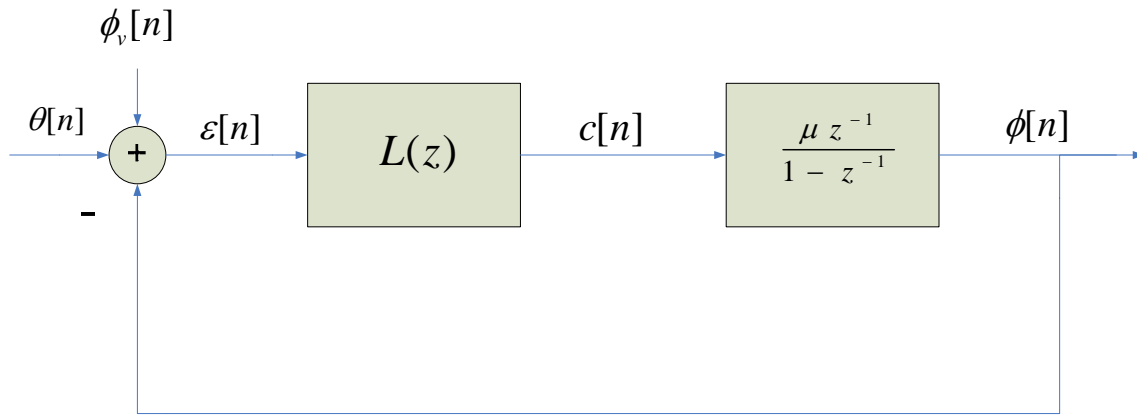


Figure 5-1 Linear model of discrete time PLL

The control signal $c[n]$ updates the phase angle $\phi[n]$ using the update equation

$$\phi[n+1] = \phi[n] + \mu c[n] \quad (5.2)$$

where μ is the step size parameter. Taking the z-transform of both sides

$$\begin{aligned} \frac{\Phi(z)}{C(z)} &= \frac{\mu}{z-1} \\ &= \frac{\mu z^{-1}}{1-z^{-1}} \end{aligned} \quad (5.3)$$

The transfer function between the input and the output, i.e. the phase transfer function of the discrete time PLL is given by

$$\begin{aligned}
 H(z) &= \frac{\Phi(z)}{\Theta(z)} \\
 &= \frac{\mu z^{-1} L(z)/(1-z^{-1})}{1 + \mu z^{-1} L(z)/(1-z^{-1})} \\
 &= \frac{\mu L(z)}{\mu L(z) + z - 1} \tag{5.4}
 \end{aligned}$$

Ignoring $\phi_v[n]$, the z-transform of the error is

$$E(z) = \frac{(z-1)\Theta(z)}{\mu L(z) + z - 1} \tag{5.5}$$

and by the rearrangement of the above equation, we obtain the phase error transfer function

$$G(z) = \frac{z-1}{\mu L(z) + z - 1} \tag{5.6}$$

5.2.1 Second Order PLL

For the second order discrete PLL, the loop filter $L(z)$ can be represented by

$$L(z) = K_L \frac{1 + \alpha z^{-1}}{1 + \beta z^{-1}} \tag{5.7}$$

Substitute the above equation in (5.4) and we obtain

$$H(z) = \frac{\mu K_L (1 + \alpha z^{-1}) z^{-1}}{1 + (\mu K_L + \beta - 1) z^{-1} + (\mu K_L \alpha - \beta) z^{-2}} \tag{5.8}$$

Further analysis [23] shows that the steady state error of the second order discrete PLL will approach zero only when $\beta = -1$. For this value, (5.8) reduces to

$$L(z) = K_L \frac{1 + \alpha z^{-1}}{1 - z^{-1}} \tag{5.9}$$

The pole at $z = 1$ in the loop filter implies that it includes an integrator stage. The constants K_L and α can be expressed as

$$\alpha = -\frac{2\zeta}{2\zeta + \omega_n T_s} \quad (5.10)$$

$$K_L = \omega_n^2 T_s + 2\zeta \omega_n \quad (5.11)$$

This is the PLL scheme we are going to use in our OFDM system to recover the residual error introduced due to an imperfect channel estimate for QPSK modulation.

5.3 Recovery Algorithm

Here we look at the phase recovery algorithm that compensates the phase introduced in the samples in proportion to their order in time domain.

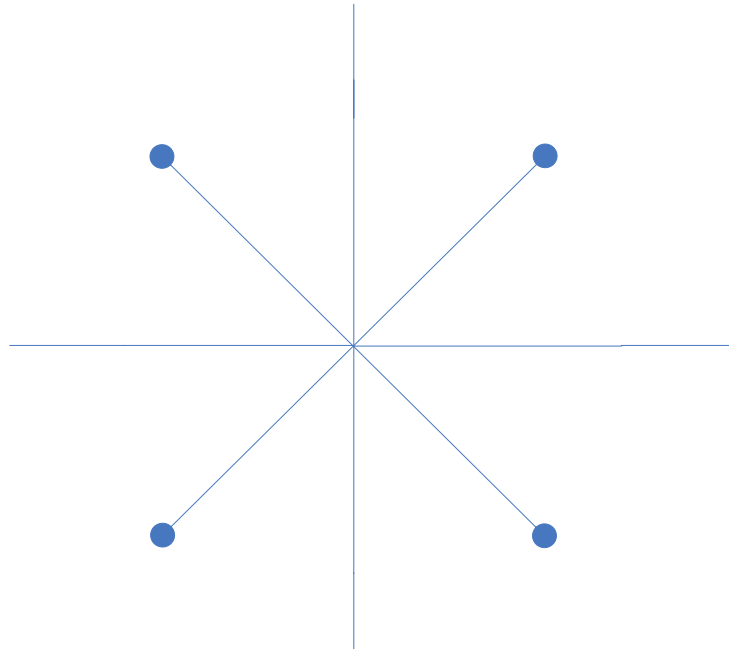


Figure 5-2 QPSK Constellation

The figure represents an ideal QPSK constellation. The received constellation assuming no error at all for QPSK is equivalent to the above figure. For a complex number raised to the power of 4, we observe

$$x^4(t) = x_R^4(t) + x_I^4(t) - 6x_R^2(t)x_I^2(t) + j2x_R(t)(x_R^2(t) - x_I^2(t)) \quad (5.12)$$

It is clear from this expression that for an ideal QPSK constellation, the imaginary part in the above equation would be zero i.e. an ideal QPSK data point raised to power of 4 will produce a number with only a real part. We use this property to correct the phase for our disturbed data points, disturbed by the residual phase error. For a point which is offset from the ideal behavior, when raised to power 4, we have the imaginary part that is the correction for the disturbed data point. This imaginary part, designated as the *Phase Correction*, then drives the loop filter of our PLL. The constants for the loop filter can be determined from (5.10) and (5.11). The output of the loop filter is the final correction needed for the recovery of the next sample. This proceeds by the reason that the samples are offset from their ideal locations by an error that increases in proportion to their place on the time scale.

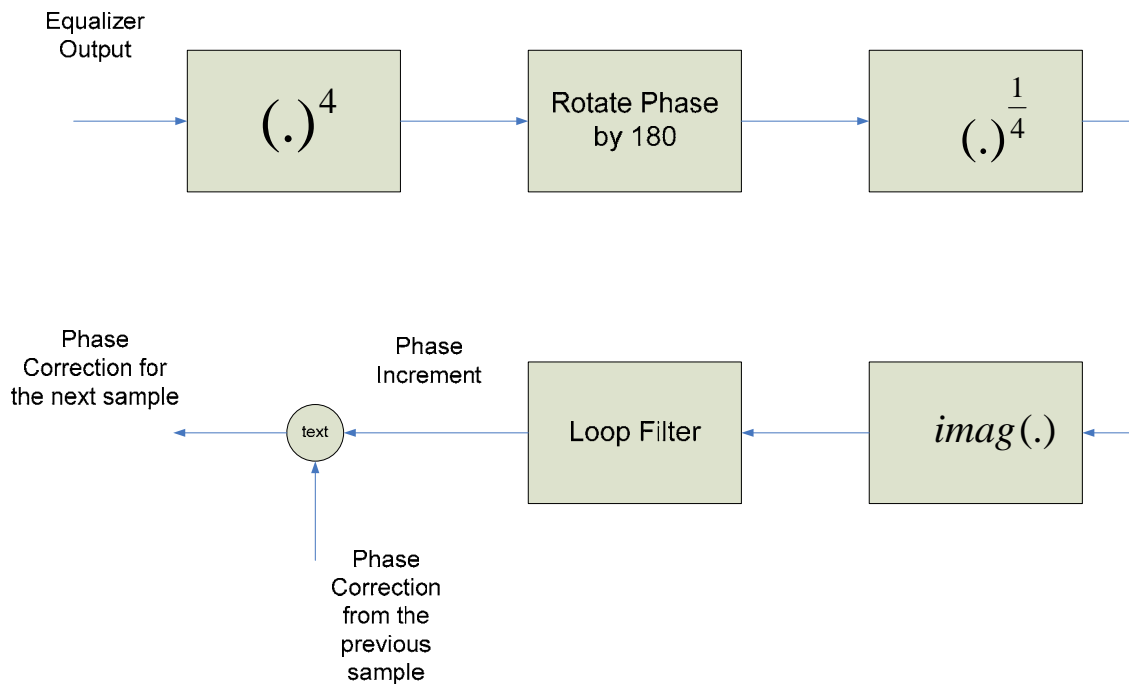


Figure 5-3 Phase recovery mechanism

The block diagram shows that the data points after equalization are fed to the fourth power operator. The assumption here is the same that a perfectly located QPSK point will produce a zero imaginary component when it is raised to power four. The complex data point is returned back to its original shape through a power of $1/M$ after giving it a shift of 180° . The imaginary part, if any, so obtained is the error by which the complex data point is shifted from its ideal location.

The phase error is then passed to the loop filter of the PLL and it generates the necessary correction for the next sample point.

Chapter 6

Channel Characteristics

The mobile channels in use today frequently experience multipath and other Doppler spread degradations. These degradations can be characterized in certain categories [23].

6.1 Mobile Channel Characteristics

Wireless mobile communications are characterized by two types of fading effects: Large scale fading and small scale fading. The average signal power attenuation due to motion over large areas is called large scale fading. Its statistics express the path loss as a function of distance. Small scale fading is the phenomenon of changes in the signal amplitude and phase due to small changes in the spatial separation between the transmitter and the receiver. This type of fading is constituted of two mechanisms: time spreading of the channel and time variant nature of the channel. In this context, few terms are worth defining; Delay spread, Coherence Bandwidth, Doppler spread, and Coherence time.

Delay Spread is a type of distortion that is caused when an identical signal arrives at different times at its destination. The signal usually arrives in a number of different paths and with different angles of arrival. The time difference between the arrival moment of the first multipath component, usually the line of sight component, and the last one, is called delay spread.

Coherence bandwidth is a statistical measure of the range of frequencies over which the channel can be considered “flat” i.e. a channel which passes all spectral components with approximately equal gain and linear phase. In other words, coherence bandwidth is the range of

frequencies over which two frequency components have a strong potential for amplitude correlation.

Doppler spread B_D is a measure of the spectral broadening caused by the time rate of change of the mobile radio channel and is defined as the range of frequencies over which the received Doppler spectrum is essentially non-zero. When a pure sinusoidal tone of frequency f_c is transmitted, the received signal spectrum, called the Doppler spectrum, will have components in the range $f_c - f_d$ to $f_c + f_d$, where f_d is the Doppler shift. The amount of spectral broadening depends on f_d which is a function of the relative velocity of the mobile, and the angle θ between the direction of motion of the mobile and direction of arrival of the scattered waves.

Coherence Time is the time interval during which two data points spaced by a certain distance in time experience sufficient correlation after passing through the channel. In other words, it is the measure of the staticness of the channel. Typically for mobile communications, it is defined as

$$T_c = \frac{0.423}{f_d} \quad (6.1)$$

6.2 Fading due to Multipath Effects

6.2.1 Flat Fading

In this type of fading, the multipath structure of the channel is such that the spectral characteristics of the transmitted signal are preserved at the receiver. However, the strength of the received signal changes with time, due to fluctuations in the gain of the channel caused by multipath.

If the channel gain changes over time, a change of amplitude occurs in the received signal. Over time, the received signal $r(t)$ varies in gain, but the spectrum of the transmission is preserved. In

a flat fading channel, the reciprocal bandwidth of the transmitted signal is much larger than the multipath time delay spread of the channel, and $h_b(t, \tau)$ can be approximated as having no excess delay (i.e. a single delta function with $\tau = 0$). Flat fading channels are also known as *amplitude varying channels* and are sometimes referred to as *narrow band channels*, since the bandwidth of the applied signal is narrow as compared to the channel flat fading bandwidth. Hence, a signal undergoes flat fading if

$$B_s \ll B_c \quad (6.2)$$

$$\text{and } T_s \ll \sigma_\tau$$

Where T_s is the reciprocal bandwidth (e.g. symbol period) and B_s is the bandwidth, respectively, of the transmitted modulation, and σ_τ and B_c are the rms delay spread and coherence bandwidth, respectively, of the channel.

6.2.2 Frequency Selective Fading

Frequency selective fading is due to the time dispersion of the transmitted symbols within the channel. Thus the channel includes *intersymbol interference (ISI)*. Viewed in the frequency domain, certain frequency components in the received signal spectrum have greater gains than others.

For frequency-selective fading, the spectrum $S(f)$ of the transmitted signal has a bandwidth which is greater than the coherence bandwidth B_c of the channel. Viewed in the frequency domain, the channel becomes frequency selective, where the gain is different for different frequency components. Frequency selective fading is caused by multipath delays which approach or exceed the symbol period of the transmitted symbol. Frequency selective fading channels are also called wideband channels because the bandwidth of the signal $s(t)$ is wider than the bandwidth of the channel impulse response. As time varies, the channel varies in gain and phase across the spectrum of $s(t)$, resulting in time varying distortion in the received signal $r(t)$. Hence, a signal undergoes frequency selective fading if

$$B_s > B_c \quad (6.3)$$

and $T_s < \sigma_\tau$

6.3 Fading effects due to Doppler Spread

6.3.1 Fast Fading

In a fast fading channel, the channel impulse response changes rapidly within the symbol duration. That is the coherence time of the channel is smaller than the symbol period of the transmitted signal. This causes frequency dispersion (also called time-selective fading) due to Doppler spreading, which leads to signal distortion. Viewed in the frequency domain, signal distortion due to fast fading increases with increasing Doppler spread relative to the bandwidth of the transmitted signal. Therefore, a signal undergoes fast fading if

$$T_s > T_c \quad (6.4)$$

$$\text{and } B_s < B_D$$

A flat fading, fast fading channel is a channel in which the amplitude of the delta function varies faster than the rate of change of the transmitted baseband signal. In the case of a frequency selective fast fading channel, the amplitude, phase, and time delays of any one of the multipath components vary faster than the rate of change of the transmitted signal. In practice, fast fading only occurs for very low data rates.

6.3.2 Slow Fading

In a slow fading channel, the channel impulse response changes at a rate much slower than the transmitted baseband signal $s(t)$. In this case, the channel may be assumed to be static over one or several reciprocal bandwidth intervals. In the frequency domain this implies that the Doppler spread of the channel is much less than the bandwidth of the baseband signals. Therefore, a signal undergoes slow fading if

$$T_s \gg T_c \quad (6.5)$$

$$\text{and } B_s \gg B_D$$

The velocity of the mobile (or the velocity of the objects in the channel) and the baseband signaling determines whether a signal undergoes fast fading or slow fading.

6.4 Guidelines for Practical System Implementation

Based on the above channel characteristics, we must keep in mind certain design criteria before implementing an OFDM based communication system. Following are some of the rules that help in realizing an OFDM transmission system.

- 1) Some of the channel characteristics must be known before designing an OFDM system. In particular, the delay spread of the channel must be known. Even if a perfect estimate is not available, as will usually be the case, we must have an approximation of the maximum expected channel delay spread.
- 2) The guard interval must be used so that its duration is longer than the maximum expected channel delay spread. This is essential so that the transient response of the channel dies down within the duration of the guard interval and the data symbols can be demodulated from the steady state response of the channel. In addition, if the guard interval is shorter than the delay spread, there will be interference between the successive symbols in an OFDM frame.
- 3) OFDM allows us to keep the duration of a symbol much greater than the delay spread to achieve flat fading. We must make sure that this condition is satisfied. It also allows us to calculate the number of carriers needed to achieve symbol duration sufficiently greater than the maximum expected channel delay spread.
- 4) However, the number of carriers must be chosen carefully since if we use a large number of carriers, the spacing between them will decrease for a given limited bandwidth. If we pack a large number of carriers in this given bandwidth, a small frequency offset will result in ICI and performance degradation.
- 5) For mobile communications, we want to avoid fast fading. We can determine the coherence time of the channel according to the maximum vehicle speed we are designing for. The constraint here for slow fading as explained earlier is that we must make sure

that our entire OFDM frame must pass through the channel within the coherence time so that the channel does not change much over the duration of the entire frame. Only then, the channel estimation and other parameters delivered by the training symbol appended at the start will be valid. Hence, this defines an upper limit on the number of symbols than can be safely transmitted through the channel.

- 6) PAPR is a major problem with OFDM systems and there must be some way by which it can be reduced. In this respect, use of a sequence that lowers the PAPR can be explored for the training sequence.
- 7) OFDM has been found to be sensitive to coding rates. So a designer has to use code rates that deliver highly reliable performance and maintain the desired throughput as well.

These are just some of the basic guidelines that have to be catered for before an OFDM transmission system can be realized. As it can be gauged, many of these issues are inter-related and hence a compromise has to be made in conflicting scenarios.

7.2.2 Phase Recovered OFDM

OFDM Receiver

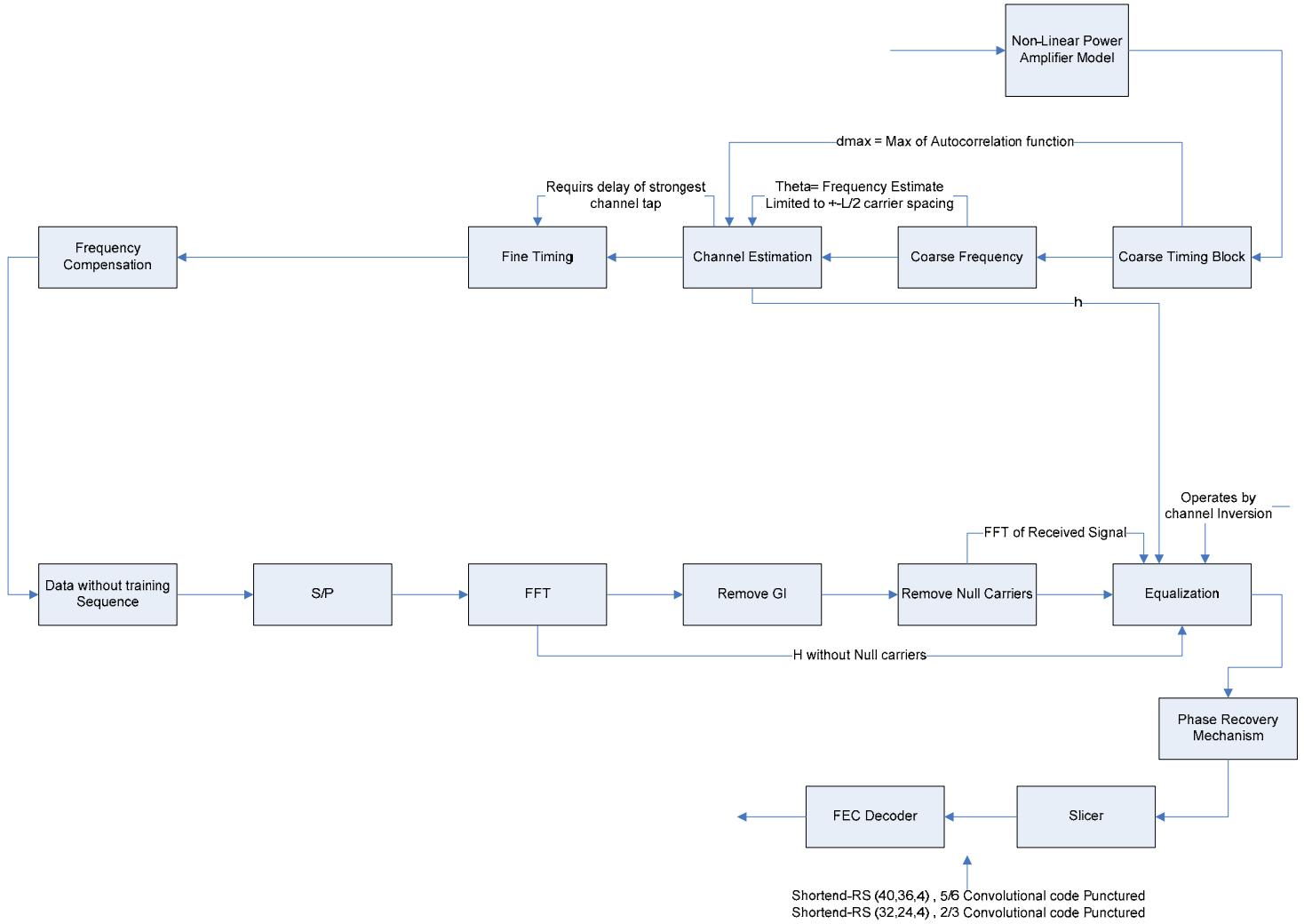


Figure 7-3 Receiver with Phase Recovery

7.3 Design Parameters

Following are the design parameters used.

Maximum Vehicle Speed Considered : $f_d = 140\text{km / hr}$

Coherence Time : $T_c = 0.423 / f_d$

Maximum Delay Spread : $\sigma_\tau = 15\mu\text{s}$ (worst case scenario [23])

Guard Interval Duration : $T_g = \sigma_\tau$

Symbol Duration : $T_s = 10\sigma_\tau$

Number of Carriers : $N = 32$

Active Carriers : $N_u = 24$

Channel Types : a) Static Rayleigh Faded (three path)

b) Mobile Rayleigh Faded (three path)

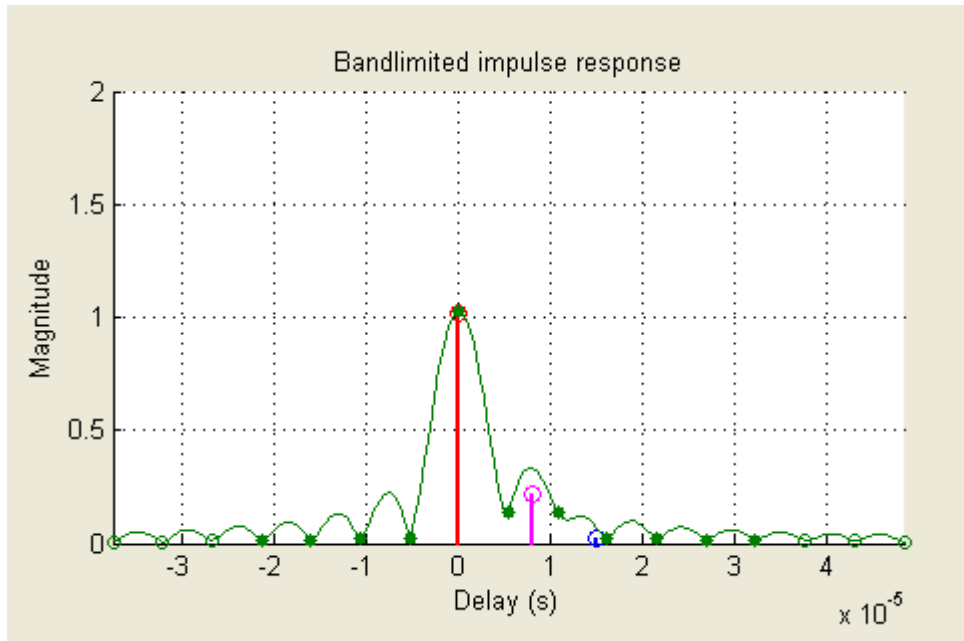


Figure 7-4 Multipath channel impulse response

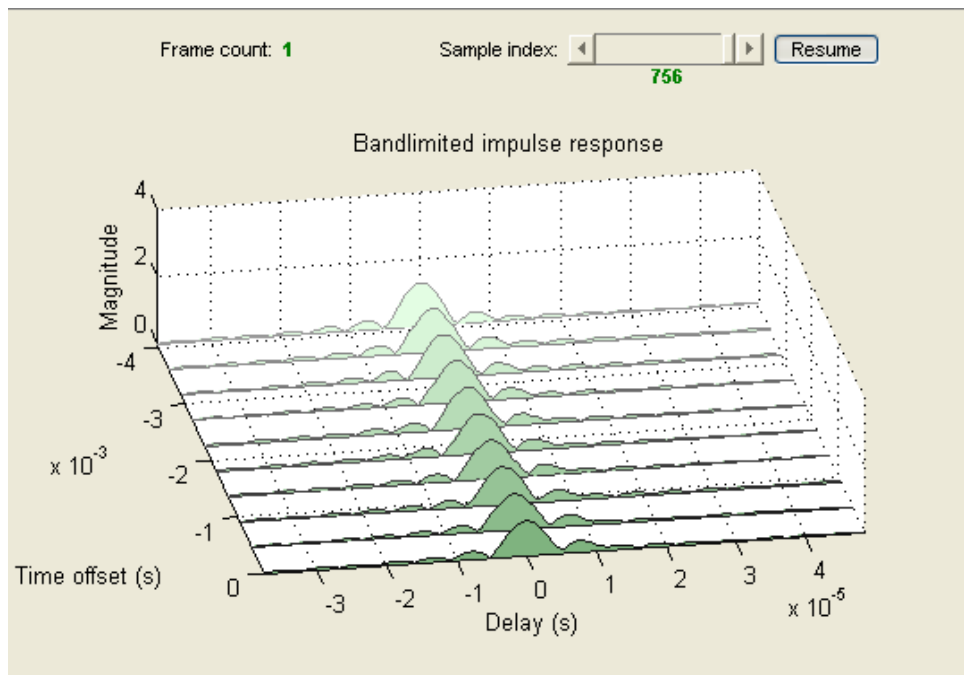


Figure 7-5 Waterfall

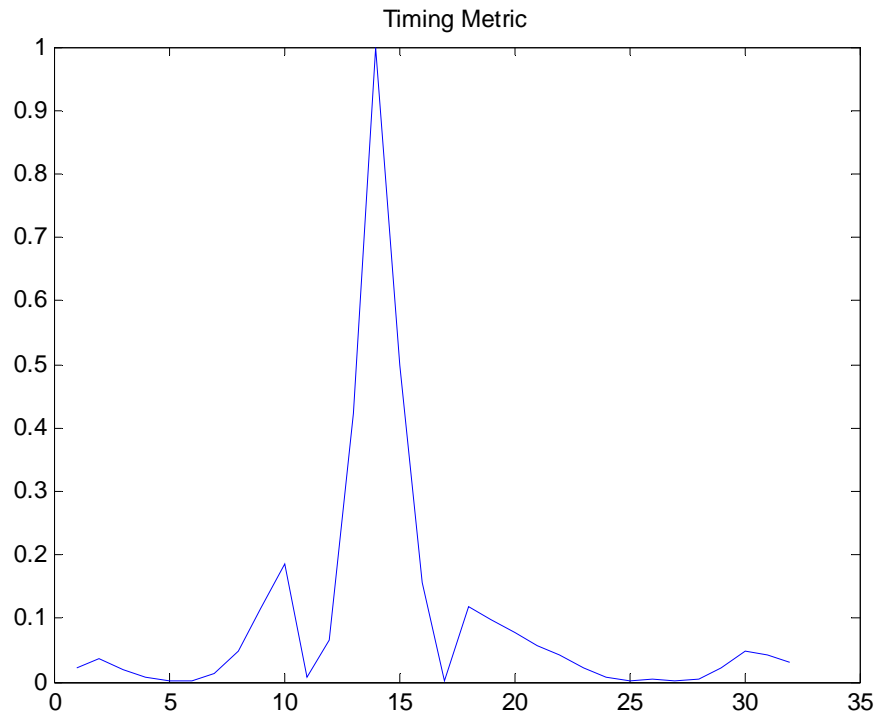
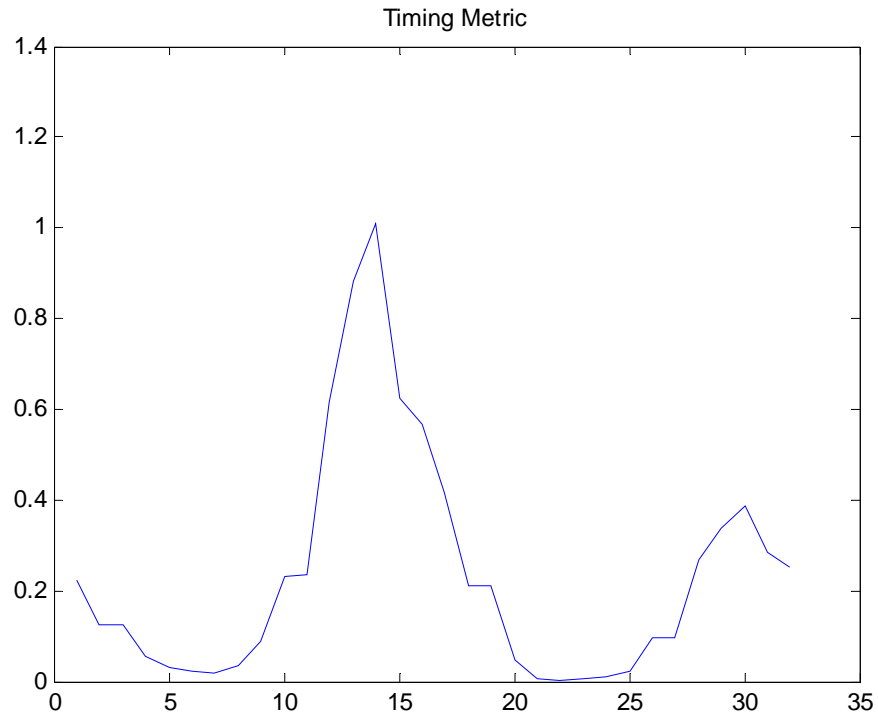


Figure 7-6 Timing metric obtained for L=4, L=8

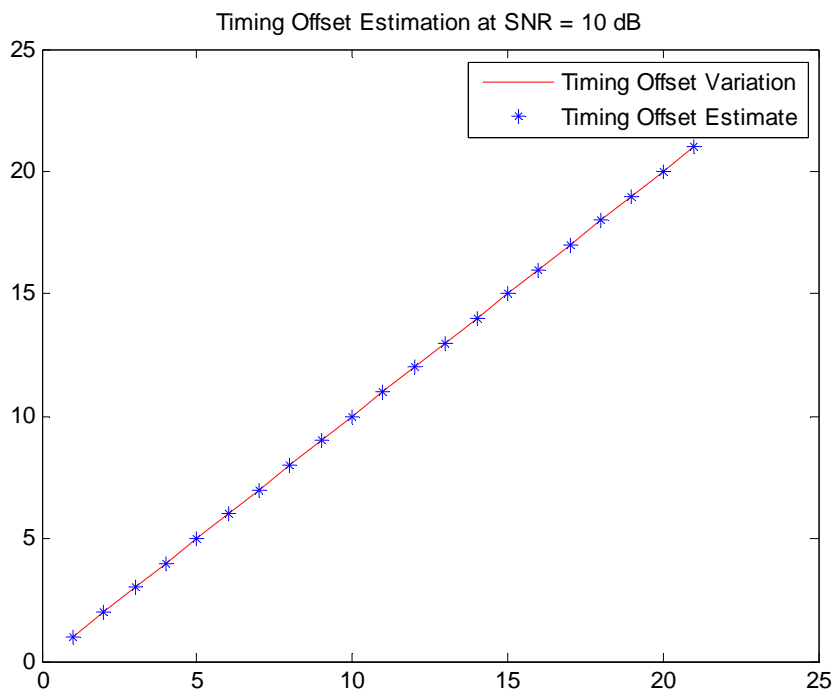
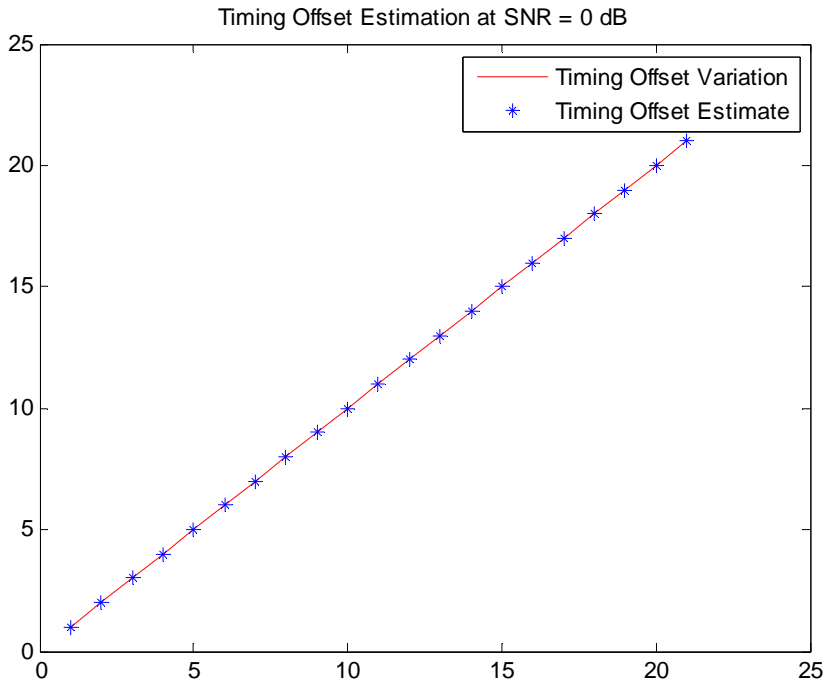


Figure 7-7 Timing Offset Estimation

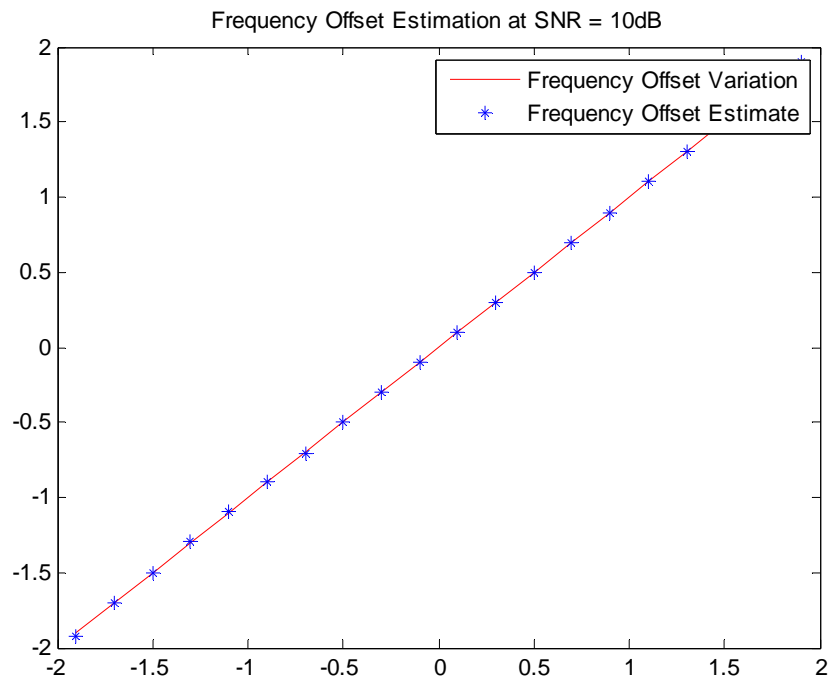
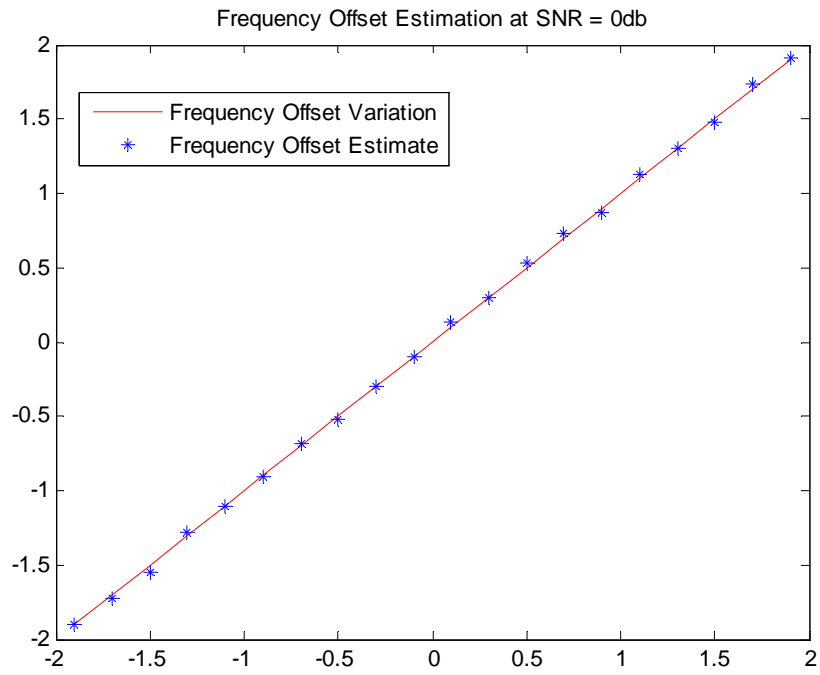


Figure 7-8 Frequency Offset Estimation

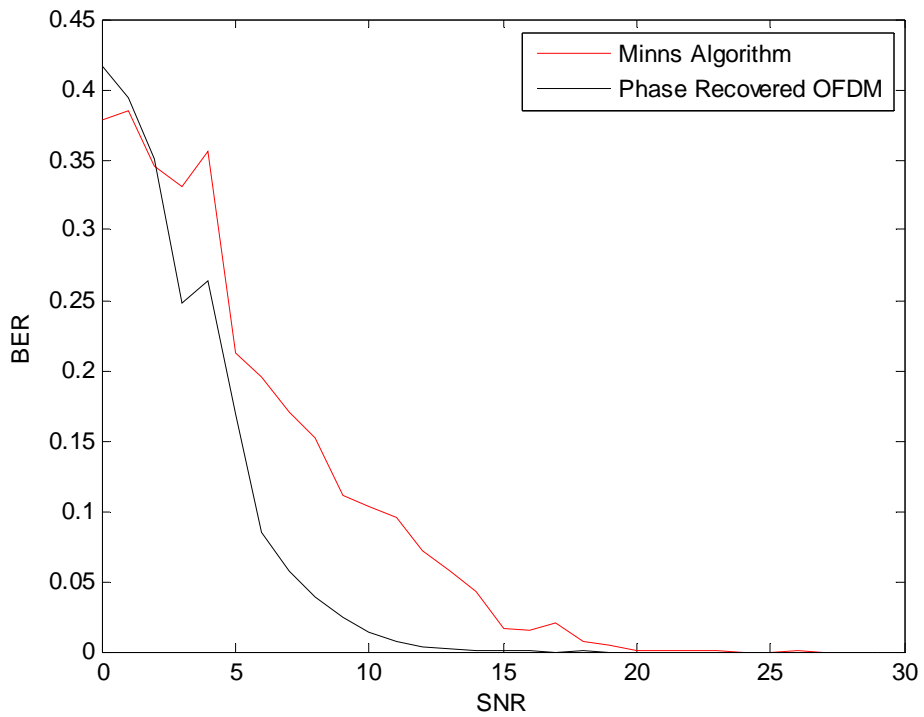
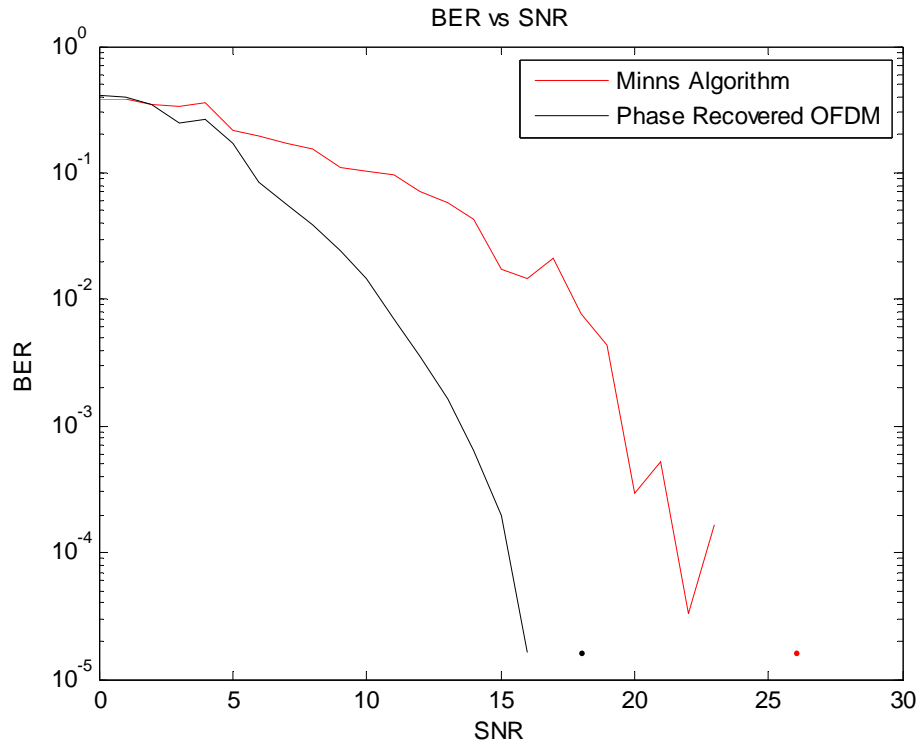


Figure 7-9 Performance Comparison in Rayleigh Faded Channel. Doppler 50 Hz

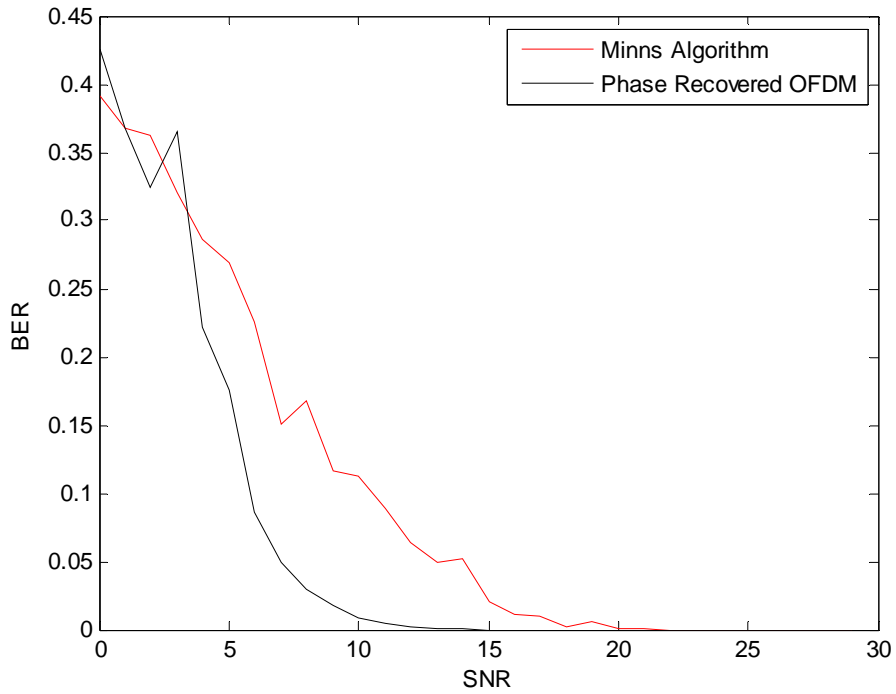
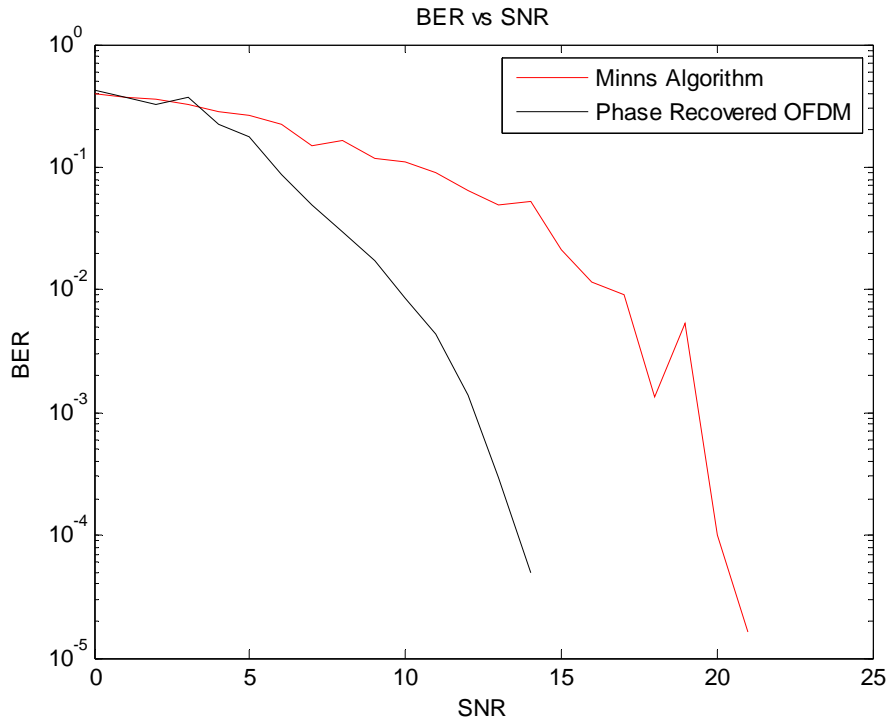


Figure 7-10 Performance Comparison in Static Rayleigh Faded Channel

Chapter 8

Conclusions

This work evaluates different synchronization strategies currently used for OFDM systems. We have seen the degradations caused by the timing and frequency offsets on a practical OFDM system. If these offsets are not compensated properly, the performance of an OFDM system is severely compromised. It was investigated that the timing metric obtained from Schmidl's scheme results in a plateau which causes uncertainty with regards to the start of an OFDM symbol. Hence the operation of OFDM may be invoked at the wrong instant and this produces interference between successive OFDM symbols. This uncertainty also causes large offset estimation variance and hence the performance of an OFDM system degrades rapidly. The frequency error estimation is also adversely affected whenever we make an error in timing synchronization. Also, if the frequency offset exceeds one carrier spacing, we have to use another training symbol to determine the integer offset. The throughput of the system, therefore, decreases and overall performance efficiency decreases.

In order to alleviate these problems, Minn and Bhargava have proposed an improved estimator. The OFDM system is implemented with a specially designed training symbol which is supplied with a sign pattern whose knowledge is common to both transmitter and receiver. This sign pattern ensures that a steep timing roll off metric is obtained. Hence the problem of uncertainty is greatly removed and an accurate estimate of the start of an OFDM symbol is obtained. An OFDM system is more sensitive to carrier frequency offset. Minn and Bhargava have proposed a coarse estimation followed by a fine estimation scheme in order to effectively evaluate the frequency offset introduced by the multipath dispersive channel. This works better than the scheme proposed by Schmidl and hence we have an improvement in performance. However, it was observed that even after a fine estimation strategy, a residual error still remains that shifts the resulting samples in an OFDM based frame. The samples are rotated by a phase that

increases in proportion to their location on the time scale. For the OFDM symbols that located at the end of the frame, this phase accumulates and there is a chance that the data points may cross their constellations and it will not be possible to decode them correctly.

To remove the rotation of the received constellation caused by this residual offset, we propose a PLL based recovery scheme that predicts the phase correction for the next sample. Although the PLL, in general, takes some time in locking the phase, but it was observed that we only need the phase correction for the previous sample to obtain the phase correction for the next sample. It proceeds by the logic that after coarse estimation, most of the error has already been removed. For the scheme proposed by Mengali, the coarse estimation process brings the phase within 0.01 of its original value. The rest of this error, instead of correcting through a fine estimation scheme, is fed to our phase recovery mechanism. We lock this proportionately increasing phase by observing that a QPSK signal raised to power 4 should ideally produce no imaginary component. The points that are offset from their optimum locations, when raised to power 4, result in an imaginary part which is given to our loop filter whose coefficients are determined to generate the desired phase correction needed.

This work proposes to eliminate the fine frequency block in the system level diagram and replace it with the phase recovery mechanism developed in this thesis. This causes a great reduction in complexity as just the information from the previous in needed to generate the phase correction for the next sample. There are no longer any equations that have to be minimized. Also, it was shown that BER improves considerably by augmenting our phase recovery block in the system structure.

8.1 Further Work

The same phase recovery process can be extended to the case of all other modulation schemes to be used in the transmission system. We can also explore the use of such sequences in our training symbol that result in a low PAPR value. The practical OFDM system is severely constrained by a high PAPR and it has limited the use of OFDM over the years. In hand held transmitters, we need to lower the PAPR so that the higher peaks in the signal can be produced by the amplifier in the transmitter.

Another interesting case would be to use this system such that the channel estimate is fed back to the transmitter. The transmitter can adapt the modulation scheme and power of the amplifier according to how good or how bad the channel is at that instant. The adaptation of the modulation scheme will allow us to deliver high data rates whenever we have a non-dispersive channel and if the conditions change, we can lower our modulation technique so that reliable transmission is ensured. On the other hand, adaptation in power of the amplifier in the transmitter will result in low interference introduced to other users in a multi-user system.

Adaptive bit loading is also being currently investigated for OFDM where each carrier or a group of carrier is modulated according to the amount of the degradation they experience in a mobile channel. The channel estimation signal can be fed back to the transmitter and then load the carries or a group of carriers based on the fading in the channel. The system considered here can be extended to develop such an adaptive bit loading strategy.

References

- [1] R. W. Chang, "Synthesis of band-limited orthogonal signals for multichannel data transmission", *Bell System Tech. J.*, 45:1775-1796, Dec. 1966.

- [2] B. R. Saltzberg, "Performance of an efficient parallel data transmission system", *IEEE Trans. Commun.*, COM-15(6): 805-811, Dec. 1967.

- [3] S. B. Weinstein, P. M. Ebert, "Data transmission by frequency-division multiplexing using the discrete Fourier transform", *IEEE Trans. Commun.*, COM-19(5): 628-634, Oct. 1971.

- [4] A. Peled, A. Ruiz, "Frequency domain data transmission using reduced computational complexity algorithms", *Proc. IEEE Int. Conf. Acoust., Speech, Signal Processing*, pages: 964-967, Denver, CO, 1980

- [5] T. Pollet, M. Van Bladel, and M. Moeneclaey, "BER sensitivity of OFDM systems to carrier frequency offset and Wiener phase noise," *IEEE Trans. Commun.*, vol. 43, pp. 191-193, Feb./Mar./Apr. 1995.

- [6] H. Steendam and M. Moeneclaey, "Sensitivity of orthogonal frequency division multiplexed systems to carrier and clock synchronization errors," *Signal Processing*, vol. 80, pp. 1217-1229, July 2000.

- [7] Michael Speth, Stefan A. Fechtel, Gunnar Fock and Heinrich Meyr, "Optimum Receiver Design for Wireless Broadband Systems Using OFDM - Part I", *IEEE Trans. Commun.*, vol. 47, No. 11, November 1999.

- [8] J.J. van de Beek, M. Sandell and P.O. B"orjesson, "ML estimation of time and frequency offset in OFDMsystems," *IEEE Trans. Signal Processing*, vol. 45, pp. 1800-1805, July 1997.

- [9] B. Picinbono, "On Circularity," *IEEE Trans. Signal Processing*, vol. 42, pp. 3473-3482, December 1994.
- [10] T.M. Schmidl and D.C. Cox, "Robust frequency and timing synchronization for OFDM," *IEEE Trans. Commun.*, vol. 45, December 1997.
- [11] H. Minn, M. Zeng, and V. K. Bhargava, "On timing offset estimation for OFDM systems," *IEEE Commun. Lett.*, vol. 4, pp. 242-244, July 2000.
- [12] H. Minn, V.K. Bhargava, and K.B. Letaief, "A robust timing and frequency synchronization for OFDM systems," *IEEE Trans. Wireless Commun.*, vol. 2, pp. 822-839, July 2003.
- [13] A. R. S. Bahai and B. R. Saltzberg, "Multi-Carrier Digital Communications. Theory and Applications of OFDM," *Kluwer Academic Publishers*, 1999.
- [14] J. S. Chow, J. C. Tu and J. M. Cioffi, "A discrete multitone transceiver system for HDSL applications," *IEEE J. Select. Areas Commun.* vol 9, pp 895-908, August 1991.
- [15] A. Ruiz, J. M. Cioffi and S. Kasturia, "Discrete multiple tone modulation with coset coding for the spectrally shaped channel," *IEEE Trans. Commun.* vol 40, pp 1012-1029, June 1992.
- [16] J. M. Cioffi, "Very high-speed digital subscriber lines (VDSL)," *Proc. Of ISCAS*, pp 590-594, May/June 1998
- [17] K. Taura, M. Tsujishita, M. Takeda, H. Kato, M. Ishida, "Digital audio broadcasting (DAB) receiver," *IEEE Trans. Cons. Electronics*, vol. 42, pp. 45-66, March 1996.
- [18] M. Russell and G. L. Stuber, "Terrestrial digital video broadcasting for mobile reception using OFDM," *Wireless Personal Commun.*, vol. 2, pp 45-66, March 1995.

[19] Tilde Fusco, “Synchronisation Techniques for OFDM systems”, Universita Degli Studi Di Napoli Federico II, 2005

[20] Yasamin Mostofi, “Timing Synchronisation and ICI mitigation for pilot aided OFDM mobile systems”, Stanford University, 2003.

[21] T. Pollet and M. Moeneclaey, “Synchronizability of OFDM signals,” in Proc. *GLOBECOM 1995*, pp. 2054-2058, November 1995.

[22] P. H. Moose, “A technique for orthogonal frequency division multiplexing frequency offset correction,” *IEEE Trans. Commun.*, vol. 42, pp. 2908- 2914, October 1994.